Chapter 3

Mean-Field to Tricritical Cross-over Behaviour near the A–C* Tricritical Point

3.1 Introduction

Experimental studies on Tricritical Points(TCP)[1] are of great current interest in not only liquid crystalline systems, but for understanding the critical plienomena associated with the condensed matter systems as a whole. In fact, the symmetry of tlie phases involved make some of the liquid crystalline transitions potential candidates to observe the TCP. However, the phase transitions in wliicli it had been experimentally observed were the nematic-smectic A(N-A) transition[2], tlie cliolesteric-smectic A (Cli-A) transition[3,4] etc. In these systems TCP was ohtained eitlier in the temperature-concentration[2] plane or in the temperature-pressure plane[3,4]. But, despite considerable efforts, the observation of such a point on a smectic A-smectic C(A-C) or smectic A-srnectc C* (A-C*) transition line had eluded experimenters. In this chapter, we describe the first observation of a TCP on the A-C* boundary.

As early **as** in 1937, Landau realised[5] that in a phase diagram, the point where a line of first order transitions meets another line of second order transitions is a special point. This problem was treated in a rigorous way by Griffiths[1,6] who termed tlie meeting point as a *tricritial* point (TCP). As the name suggests, TCP, by definition, is a meeting point of three critical lines. In order to discuss the TCP, let us follow the notations set forth by Griffiths for the case of He^3-He^4 mixtures. Consider the three set of conjugate variables: (i)entropy S and temperature T (ii) ordering density ψ (suyerfluid order parameter) and the ordering field η (conjugate to the order parameter). (iii) non ordering density X (mole fraction of He^3) and the non ordering field Δ (differ-

ence in chemical potentials between He^3 and He^4). The generic phase diagram in the T-η-Δ plane has the form shown schematically in Figure 3.1. The surface A in the η=0 plane is a first order (or coexistence) surface. For $T>T^*$ (T^* is the temperature corresponding to the TCP) this surface terminates on a line of critical points denoted by L. For $T<T^*$ the coexistence surface A terminates on a first order line. Further, the surface A, which lies initially in the η=0 plane, bifurcates into two surfaces ('tricritical wings') extending out into the regions $\tau < 0$ and $\tau > 0$, terminate on the critical lines L_1 and L_2. The meeting point of the tliree critical lines L, L_1 and L_2 occurs at the point P, which is called the tricritical point(TCP). Tlie coordinates of P are $P \equiv P(T=T^*, \Delta=\Delta^*, \eta=0)$. In order to obtain a TCP experimentally, one has to observe three critical lines meeting in this special manner. But in most of the systems tlie field which is conjugate to the order parameter, is a 'fictitious' field not realisable in the laboratory. (For eg., in metamagnets η is tlie staggered field). Therefore from a practical point of view, TCP in the η=0 plane can be defined as a point where a line of first order transitions changes over to a line of second order transitions (Figure 3.2). Examples of Cricritical points have been found in He^3-He^4 mixtures[7], metamagnets[8], ammonium halides[9], ferroelectrics[10,11,12] etc.

One of the main reasons for not observing the TCP on the A–C* boundary was that no concrete proof of a first order A-C/A-C* transition was obtained. Experimentally, the A-C/A-C* transition was almost always found to be second order. Not surprisingly, therefore, the first unambiguous observation of a first order transition, described in the Chapter 2, triggered the search for a TCP on tlie A-C* boundary. Another important associated problem is concerned

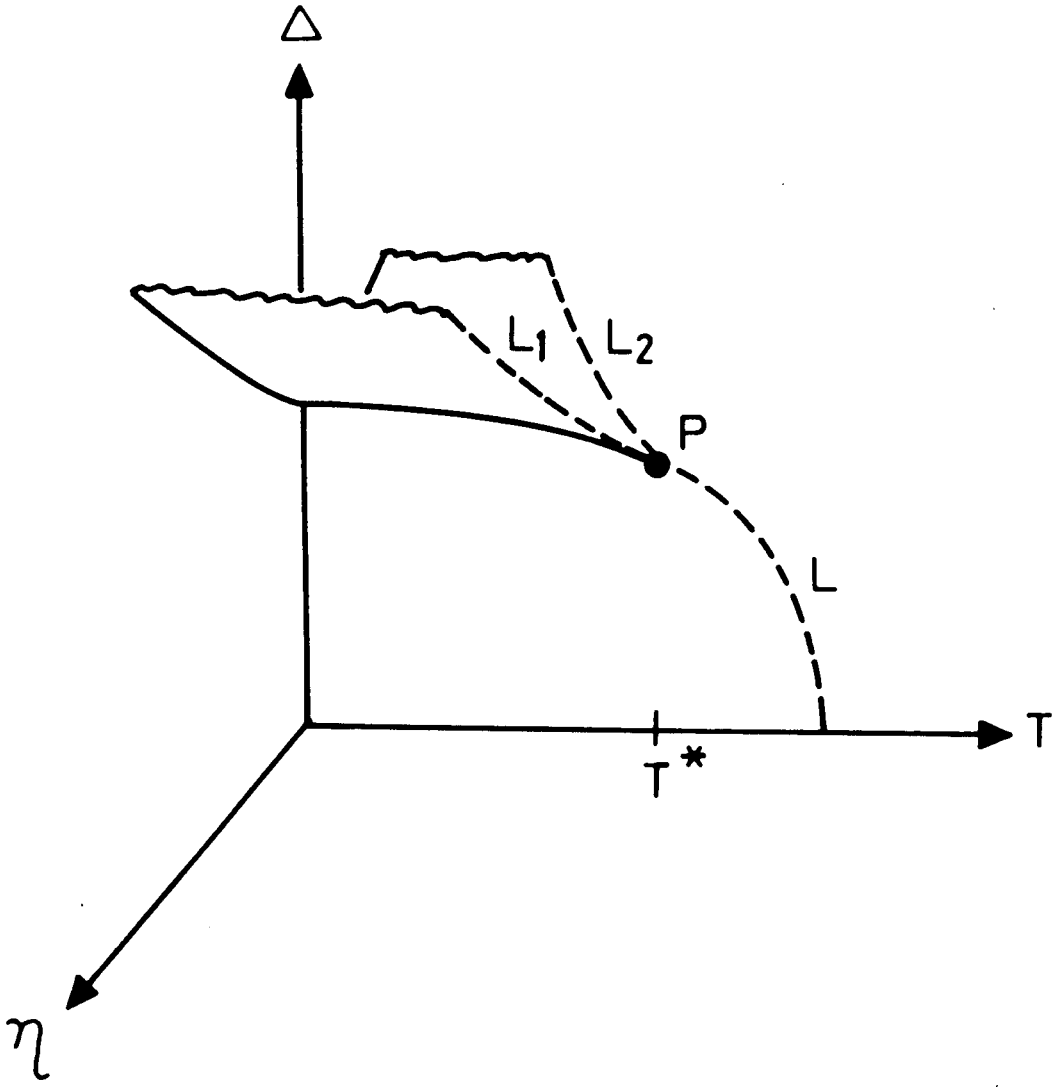

Figure 3.1: Hypothetical phase diagram for helium mixtures. Difference in chemical potentials for He^3 and He^4 is denoted by Δ wliile η is tlie fictitious ordering field. L_1, L_2 and L are tlie critical lines which meet at the point P called the *tricritical point* (TCP).

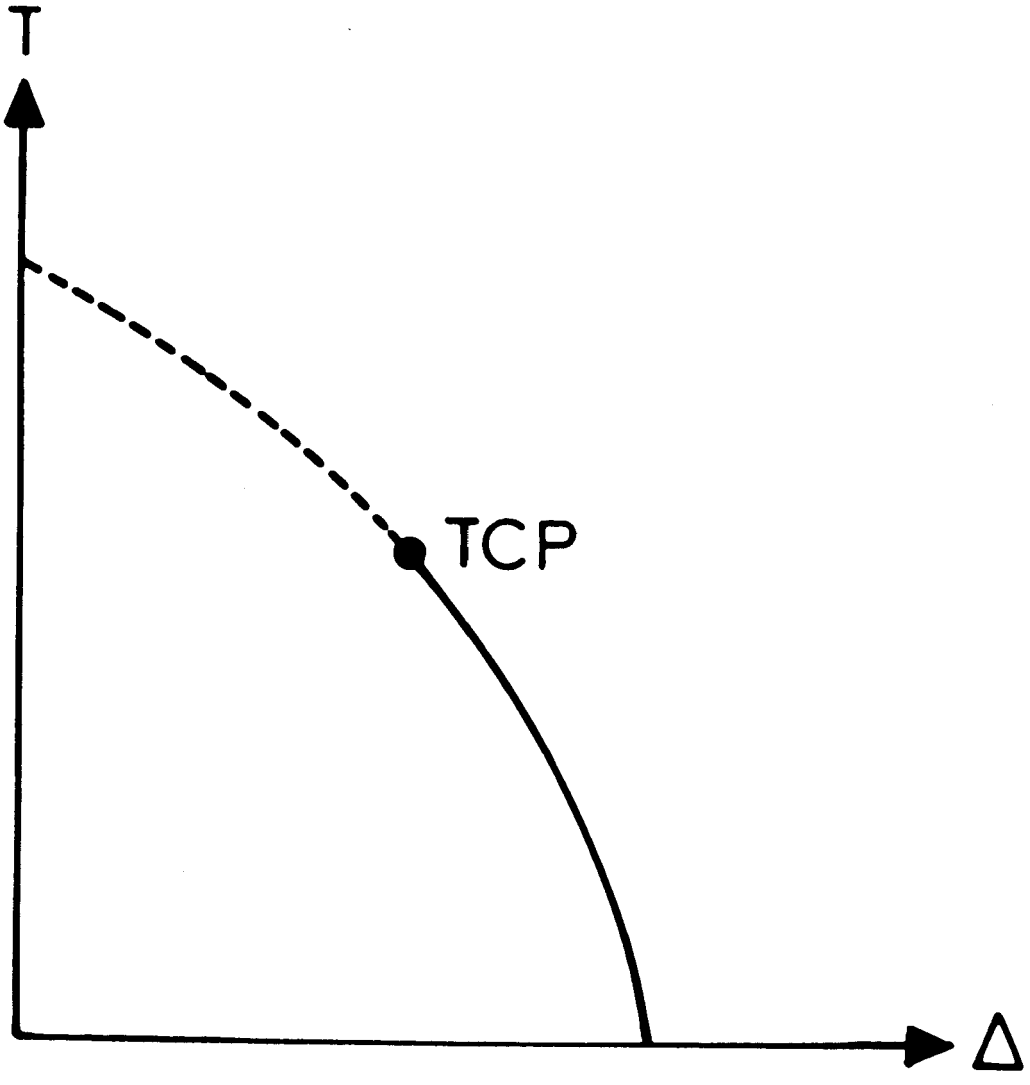

Figure **3.2:** Tricritical phase diagram in the η=0 plane. Dashed line is a line of second order transitions and solid line is a line of first order transitions.

with the exact nature of the critical behaviour of this transition, i.e., to which universality class it belongs to. de Gennes proposed[13] that, owing to the complex order parameter, the transition might exhibit helium-like (or XY class) beliaviour. Earlier experiments[14]-[18] reported the critical exponents for the A-C transitions, in particular the one for the temperature variation of the order parameter, to have a value anywhere from mean-field(MF) to XY class values. But high resolutioii studies[19] clearly demonstrated that this transition is MF like by showing that the temperature variation of the tilt angle obeys a simple power law of the type $\theta = \theta_o t^{\beta}$ (where $t = \frac{T_{AC} - T}{T_{AC}}$, T_{AC} being the A-C transition temperature and β is the critical exponent for the temperature variation of the tilt angle) and gives $\beta = 0.47 \pm 0.04$. (Note that the MF value is 0.5). The Ginzburg criterion[20] was used to calculate the width of the critical region – if it exists – over which a system sliould show the XY class behavior. The width of the critical region is given by

$$\frac{|T - T_{AC}|}{T_{AC}} = \frac{k_B^2}{32\pi^2 (\Delta C)^2 (\xi_{o\|})^2 (\xi_{o\perp})^4} \qquad (3.1)$$

where T_{AC} is the transition temperature, k_B is the Boltzmann constant, ΔC is the MF heat capacity jump at the transition, $\xi_{o\|}$ and $\xi_{o\perp}$ are the bare correlation lengths along and perpendicular to the director. For 8S5, the estimated XY-like region turns out to be narrower than 10^{-5}, i.e., $|T - T_{AC}| \simeq 3$ mK, provided $\xi_o = \xi_{o\|}^{1/3} \xi_{o\perp}^{2/3} > 13\mathring{A}$.

In a typical material ξ_o is found to be of the order of $70\mathring{A}$[21]. This means that $T\text{-}T_{AC}$ would be much smaller and therefore to observe the XY-like behaviour one has to go extremely close to T_{AC}. The value of $\beta = 0.5$, mentioned above,

is obtained as follows. The free energy density near the A-C transition can be written as,

$$F = F_o + \frac{1}{2}at\theta^2 + \frac{1}{4}b\theta^4 \tag{3.2}$$

wliere F_o is the non singular part of the free energy and θ is the order parameter for the transition (tilt angle in present case) a and b are positive constants for a second order transition. At the transition, since t = 0, the second term goes to zero. Minimising the free energy we get $0 \propto t^{0.5}$.

Anotlier important contribution in understanding this transition came from Huang and Viner[22]. Tliey realised that the generally observed heat capacity anomaly in the vicinity of the A-C* transition cannot be explained either in the frame work of the XY model or the simple mean-field model mentioned above. However, the introduction of a sixth order term[22] in the free energy expression describes the data well implying that the A-C or A-C* transition in most of the materials lies close to a mean-field TCP with a concomitant existence of a cross-over beliaviour from a mean-field-like region to a tricritical-like region[23]. This extended mean-field free energy expression is written as follows:

$$F = F_o + \frac{1}{2}at\theta^2 + \frac{1}{4}b\theta^4 + \frac{1}{6}c\theta^6 \tag{3.3}$$

where the new coefficient c is also a positive constant. From Equation **3.3,** depending on the relative values of b and c different regions can be identified, a graphical representation of which is shown in Figure **3.3.** Some important points to be noted here are,

Region (1) $b>0$ and $b \gg c \Rightarrow \beta=0.5$ i.e., a MF behaviour.

Region (2) $b>O$ and $b\sim$ c $\Rightarrow$ $0.25 < \beta < 0.5$, a value lying between MF and TCP

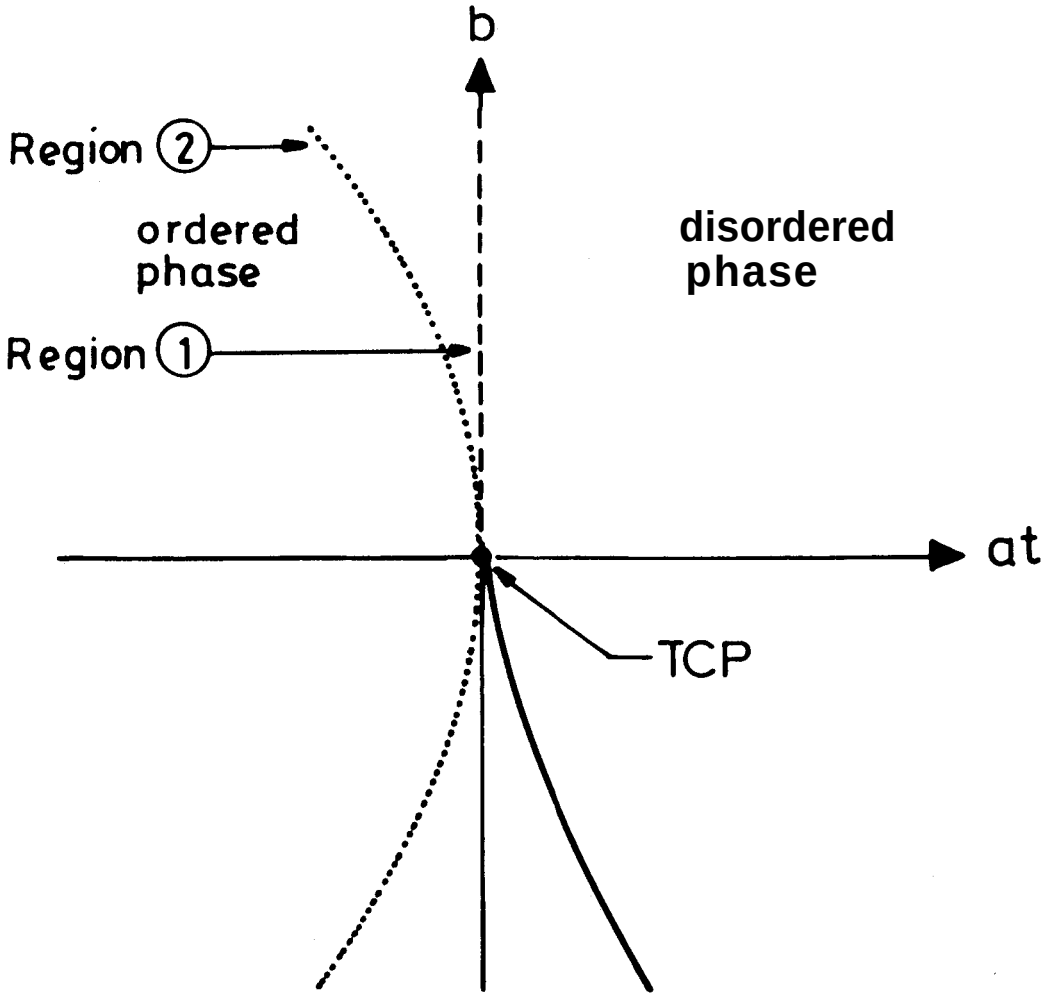

Figure **3.3:** Tricritical phase diagram in the b vs *at* plane.

values. This region is termed as tlie MF - TCP cross-over region.

Tlie domain wliere b<0 and $c>0$, shows a first order transition.

The point wliere b=0 but $c>0$ is tlie tricritical point.

Thus depending on the path of approach of tlie experiment and the proximity to TCP, one can obtain different values for tlie exponent β.

The influence of tlie TCP can be quantified as follows:

Minimising Equation 3.3 witli respect to tilt angle 6 we get,

$$\theta^2 = 0 \quad for\ T > T_{AC} \tag{3.4}$$

$$\theta^2 = \frac{b}{3c}[(1 + 3t/t_o)^{1/2} - 1] \quad \text{for } T < T_{AC} \tag{3.5}$$

where $t = \dfrac{T_{AC} - T}{T_{AC}}$ *and* $t_o = \dfrac{b^2}{ac}$.

The second derivative of tlie free energy witli respect to temperature gives tlie heat capacity jump ΔC

$$\Delta C = 0 \quad for\ T > T_{AC} \tag{3.6}$$

$$\Delta C = \frac{a^{3/2}T(T_m - T)^{-1/2}}{2(3c)^{1/2}T_{AC}^{3/2}} \text{ for } T < T_{AC} \tag{3.7}$$

wliere $T_{,,} = T_{AC}(1+t_o/3)$.

From Equation 3.5, we see that, if t $\ll$ t_o then $\theta \propto t^{0.5}$ wliicli, as seen earlier, represents a MF transition witliout any cross-over effects. If t $\gtrsim$ t_o, then $\theta \propto t^{0.25}$, which signifies a TCP. Thus, t_o is a temperature cliaracterising the MF to tricritical cross-over behaviour. A more physical definition for t_o can be given in terms of tlie specific heat curve. It is considered as the full width at lialf maximum of tlie heat capacity peak[23]. Thus tlie magnitude of t_o (wliicli in turn depends on coefficients b and c in tlie free energy expression) decides

how close the system is to the TCP and whether the concomitant existence of the mean-field to tricritical cross-over behaviour can be observed. Another important outcome of tliis analysis is tliat as the TCP is approached the range of the MF region decreases and shrinks to zero at the TCP.

After obtaining clear evidence of a first order A-C* transition in MCP7OB, (experimental characterisation of this feature have been described in Chapter 2) the next logical step was to search for a TCP. This problem reduces to the question of whether the nature of the transition can be changed to second order, for e.g., by adding a suitable second substance, with a known second order A-C transition. In tliis chapter, we present results of high precision X-ray measurements of the tilt angle on a binary liquid crystalline system which led to the first observation of a A-C* tricritical point. Detailed analysis of the associated MF to tricritical cross-over phenomena is also presented.

3.2 Experimental

The compounds used are 4-(3-methyl-2-chloropentanoyloxy)-4′- heptyloxy biphenyl (MCP7OB) and 4-heptyloxy-4′- decyloxybenzoate(7OPDOB) whose structural formulae and transition temperatures are given Table 3.1.

Note tliat MCP7OB has a cliiral C phase while the C phase of 7OPDOB is achiral. But as mentioned in Chapter 2, this does not change the physics of the topic under consideration.

Table 3.1: Structural formulae and transition temperatures (°C) of MCP7OB and TOPDOB

MCP7OB

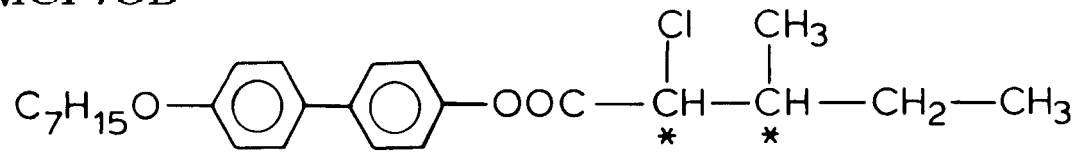

7OPDOB

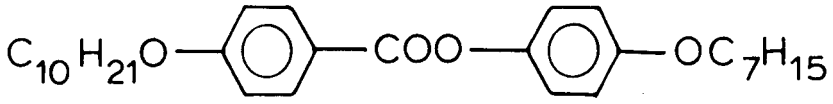

MCP7OB	Iso		A		C*		G*	
	.	**63**	.	54	.	42.2	.	
7OPDOB	Iso		N		A		C	
	.	8	.	85.1	.	80.5	.	

Iso = isotropic phase, N = nematic,

A = smectic A, C = smectic C,

C* = chiral smectic C, G* = chiral sinectic G phase.

3.2.1 X-ray studies

The X-ray diffraction experiments have been conducted using a computer controlled Guinier diffractometer. The details of the set up are given in Chapter 2 and will not be repeated here. As the purpose of the experiment was to obtain critical exponents the layer spacing data were collected at close intervals of temperature ($\sim$ a few mK) both in the A and C* phases. The tilt angle θ was calculated using the expression

$$\theta = \cos^{-1}(d_{C^*}/d_A) \tag{3.8}$$

wliere d_{C^*} and d_A are the layer spacings in C* and A phases respectively. The value of θ was cross checked by getting 'four spot' pattern,details of which are also described in Chapter 2.

3.2.2 Sample preparation

The required amounts of MCP7OB and 7OPDOB were weighed on a clean glass coverslip using a micro balance (Perkin-Elmer AD2). The sample with the coverslip was later transferred to a preheated oven. The materials were mixed thoroughly at a temperature much above the melting point of either of the materials. A small amount of sample was taken on a clean glass slide and was covered with a coverslip. This was kept inside a programmable hot stage (Mettler FP82) in conjunction with a polarising optical microscope (Leitz–Orthoplan). The temperature was varied very slowly (0.1°C/min) and the transition temperature was determined by observing the textural changes. The sharpness of the transition temperatures determined the purity and the homogeneity of the mixture.

3.3 Results and Discussion

The temperature-concentration(T-X) (where X is tlie mol% of 7OPDOB in the mixture) phase diagram for MCP7OB-7OPDOB system, obtained using optical microscopic studies, is shown in Figure 3.4.

We liave carried out X-ray diffraction experiments on several mixtures of SOPDOB in MCP7OB. Preliminary measurements were carried out on four of tliese mixtures. They are X=5.15, 9.68, 15.0 and 19.4.

As we liave already seen in Chapter 2, tlie pure MCPTOB has a first order A-C* transition. Figures 3.5(a) and (b) show the temperature variation of layer spacing and tlie intensity peak for MCP7OB. Near the transition, a two-phase region is observed wherein tlie layer spacing has two values corresponding to both A and C* phases. Also note, the cross-over of intensities of X-ray diffraction peaks. Both these features are the hallmark of a first order A-C* transition. Qualitatively, similar features obtained for X=5.15 and 9.68 indicate that the transition in tliese mixtures is also first order. Figures 3.6 (a) and (b) show the plot of layer spacing and intensity as a function of temperature for X=5.15. Here we see that the jump in the layer spacing at the transition is smaller compared to pure MCP7OB. For X=9.68, it is further reduced. Thus tlie strength of tlie first order transition decreases with increasing concentration of 7OPDOB so much so that for both X=15.0 and X=19.4 mixtures, tlie layer spacing varies continuously across the transition without any jump. Also the intensity shows a monotonic variation witli temperature. In other words, there is no two-phase coexistence region for either of these mixtures. Evidently, the transition for these

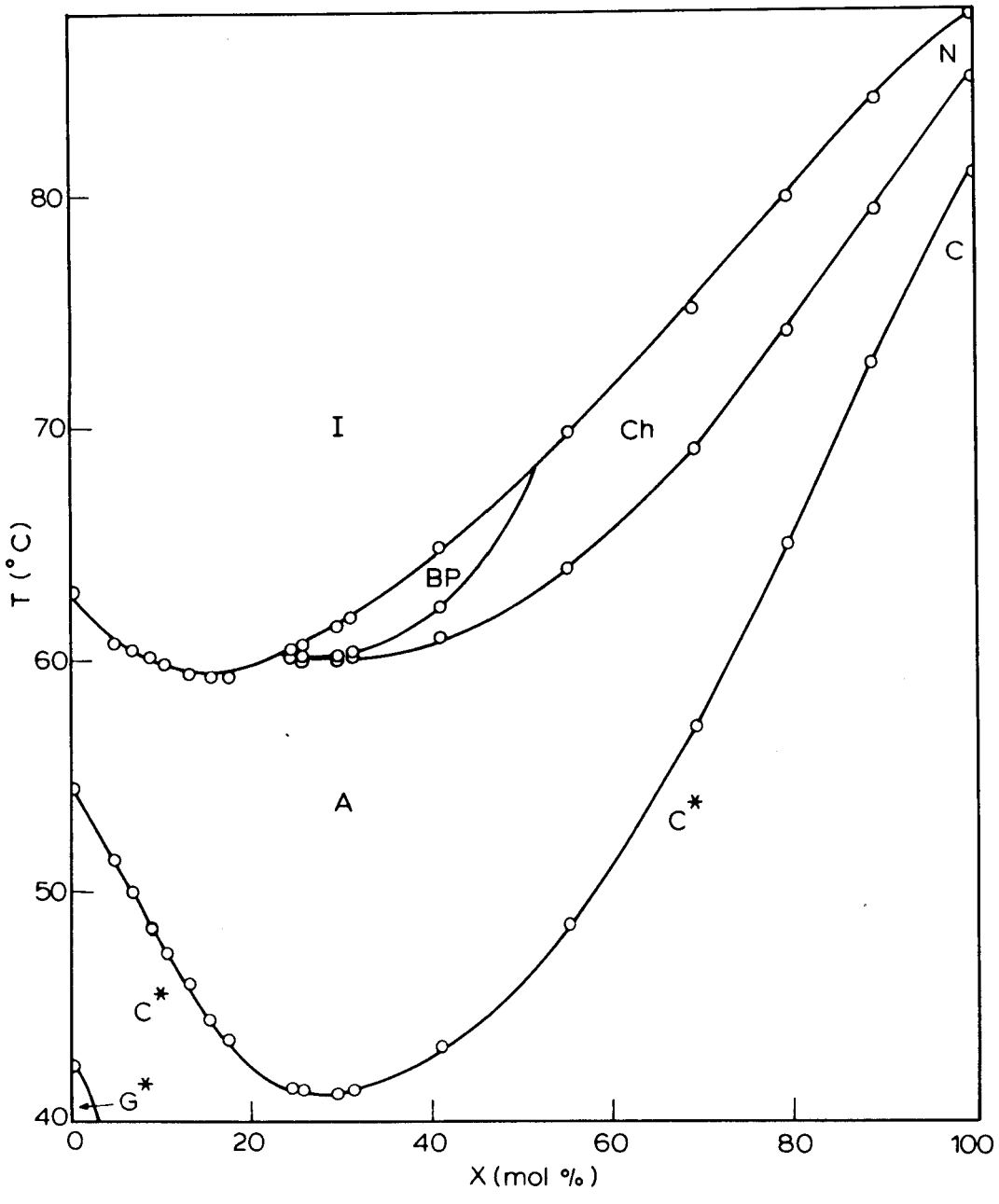

Figure 3.4: The temperature-concentration (T-X) diagram for MCP7OB–SOPDOB binary system.

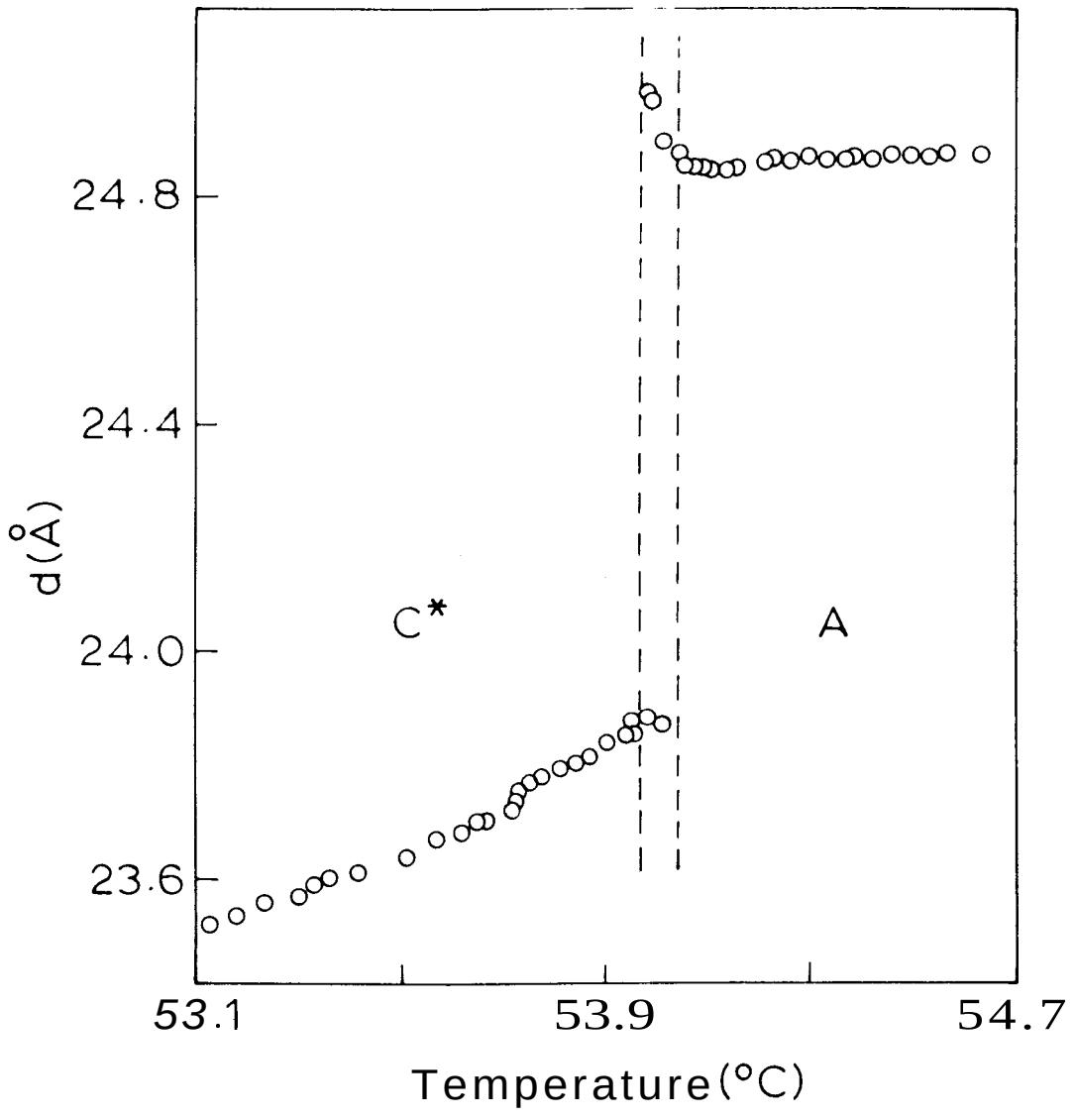

Figure **3.5:** (a) Variation of smectic layer spacing d with temperature in the vicinity of the A-C* transition in MCP70B. Tlie vertical dashed lilies enclose the two-phase region.

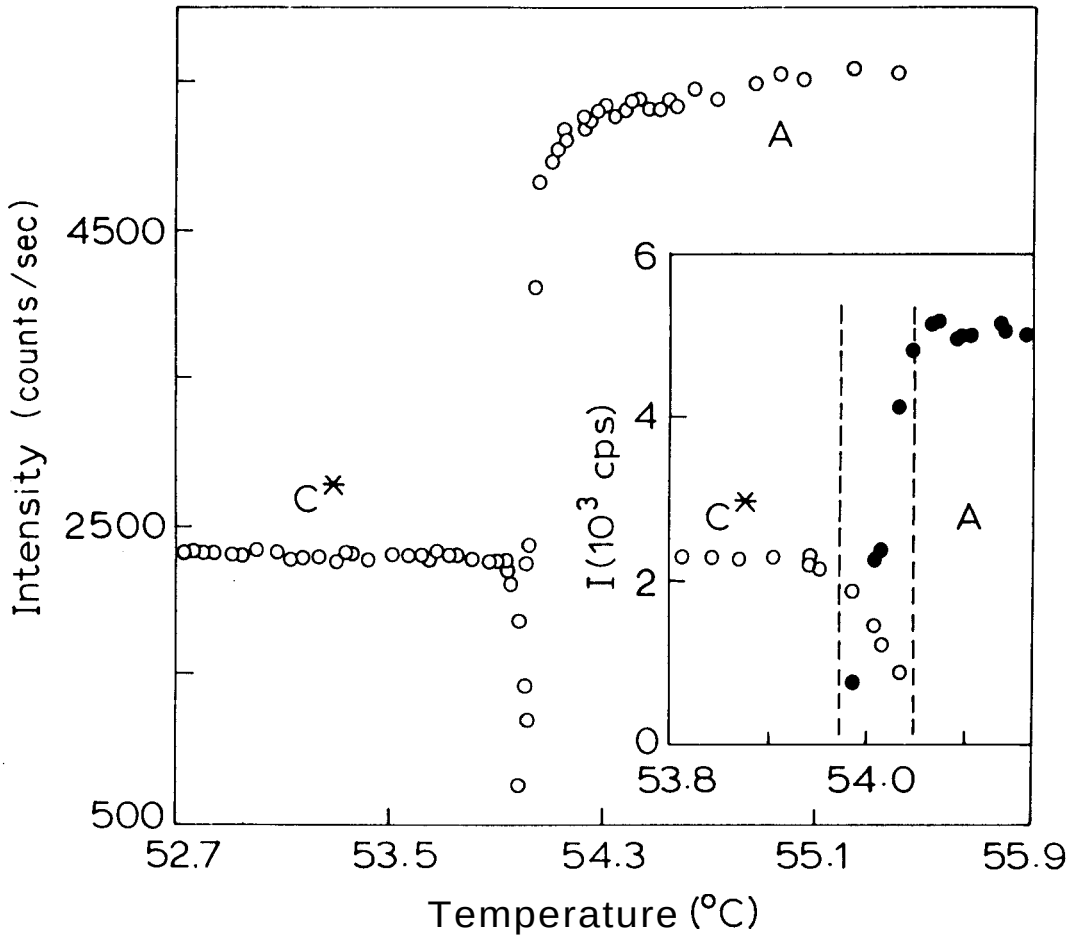

Figure **3.5:** (b) Variation of peak intensity of the X-ray diffraction maxima as a function of temperature for MCP70B. The data in the immediate vicinity of A-C* transition are shown on an enlarged scale in the inset. Solid and open circles in the inset correspond to the density modulations in the A and C* phases respectively.

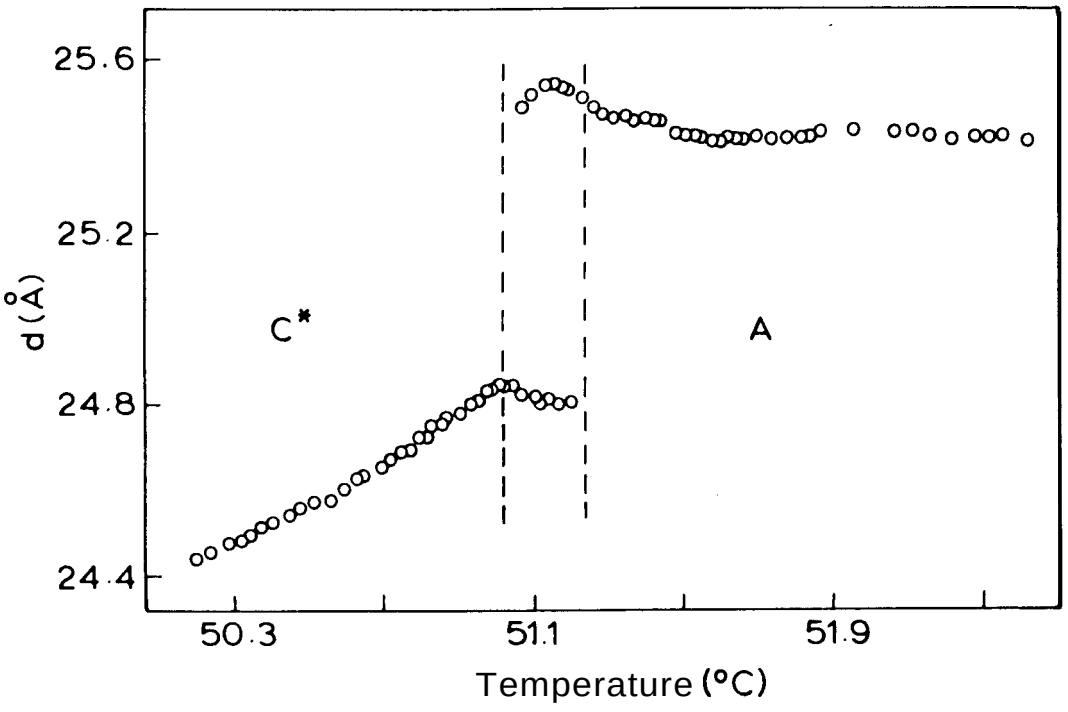

Figure *3.6:* (a) Thermal variation of smectic layer spacing near the A-C* **transition** for X=5.15.

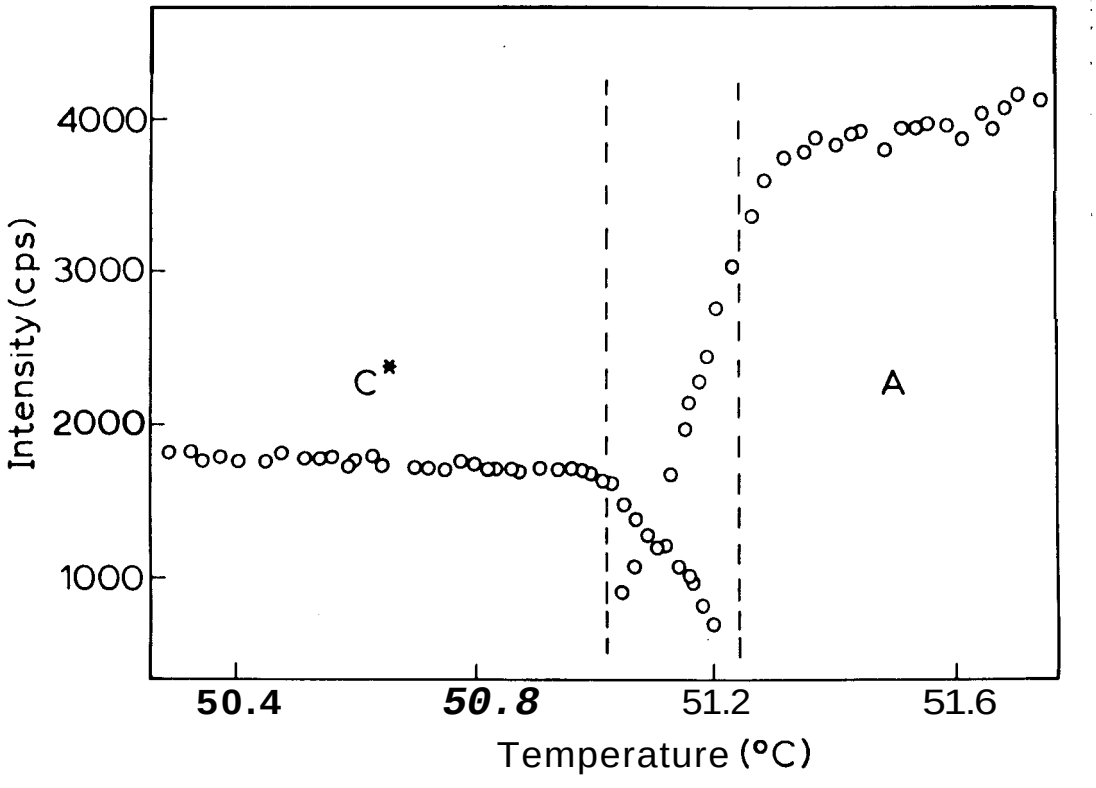

Figure 3.6: (b) The temperature variation of peak intesity for X=5.15.

mixtures is second order. Plot of the temperature variation of layer spacing and intensity for X=15.0 is given in Figure 3.7. The temperature variation of tilt angle θ determined using Equation 3.8, in the four mixtures and also in pure MCP7OB are given in Figure 3.8. It is clear that, with increasing concentration of TOPDOB, the jump in **0** at the transition decreases and finally for $X \geq 15.0$, it goes continuously to zero, indicating a change in the order of the transition from first to second order. We can therefore surmise that a TCP exists in the concentration range between X=10.0 and X=15.0.

In order to study the nature of the TCP and the concomitant cross-over phenomena, we have carried out high resolution X-ray diffraction experiments on five different mixtures, all of which lie on the second order side of the TCP. The concentrations of the mixtures used are X=16.92, 15.49, 14.02, 13.6 and 13.3.

As the Ginzburg temperatures for these materials were not known (since the specific heat or the correlation length data were not available), to ascertain the true nature of the TCP, we had to collect the data at very close intervals of temperature. During the experiment, the sample temperature was varied very slowly (100 mK/hour) and the data were collected at temperature intervals of ~5mK, the temperature being kept constant to about 2 mK during each measurement. The high precision of the data is evident from Figure 3.9 which is a representative plot of the layer spacing variation across the transition. The relative accuracy in the determination of the wave vector is reckoned to be 2×10^{-4} Å^{-1}.

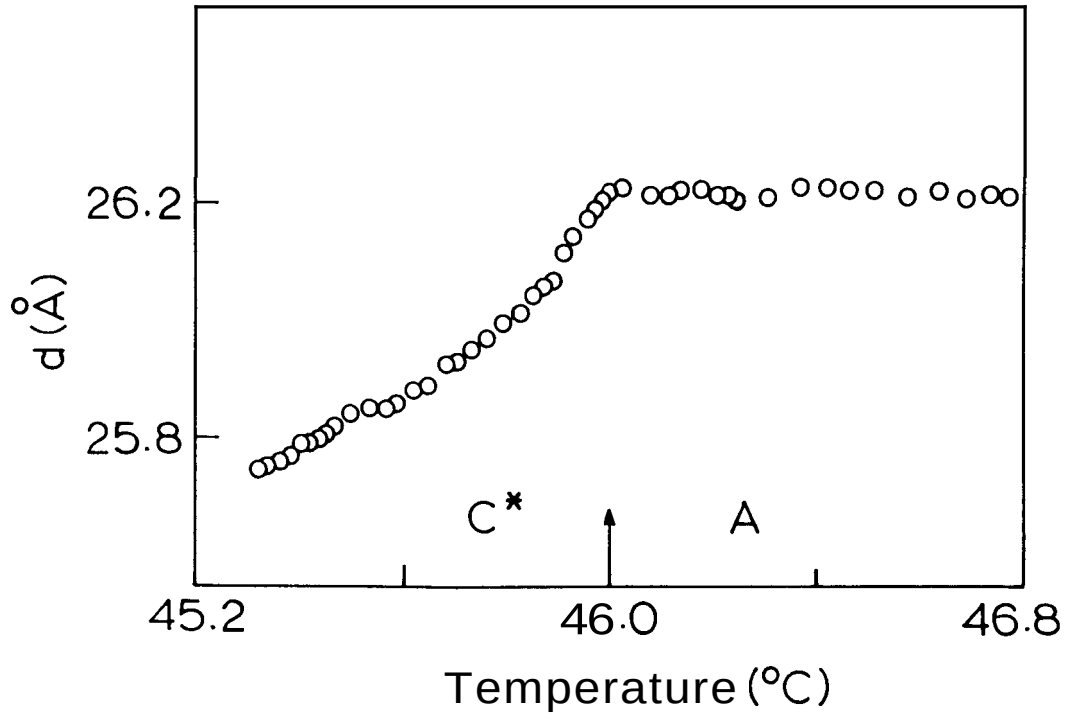

Figure **3.7:** (a) Thermal variation of d for X=15.0. The layer spacing varies continuously with temperature across the transition.

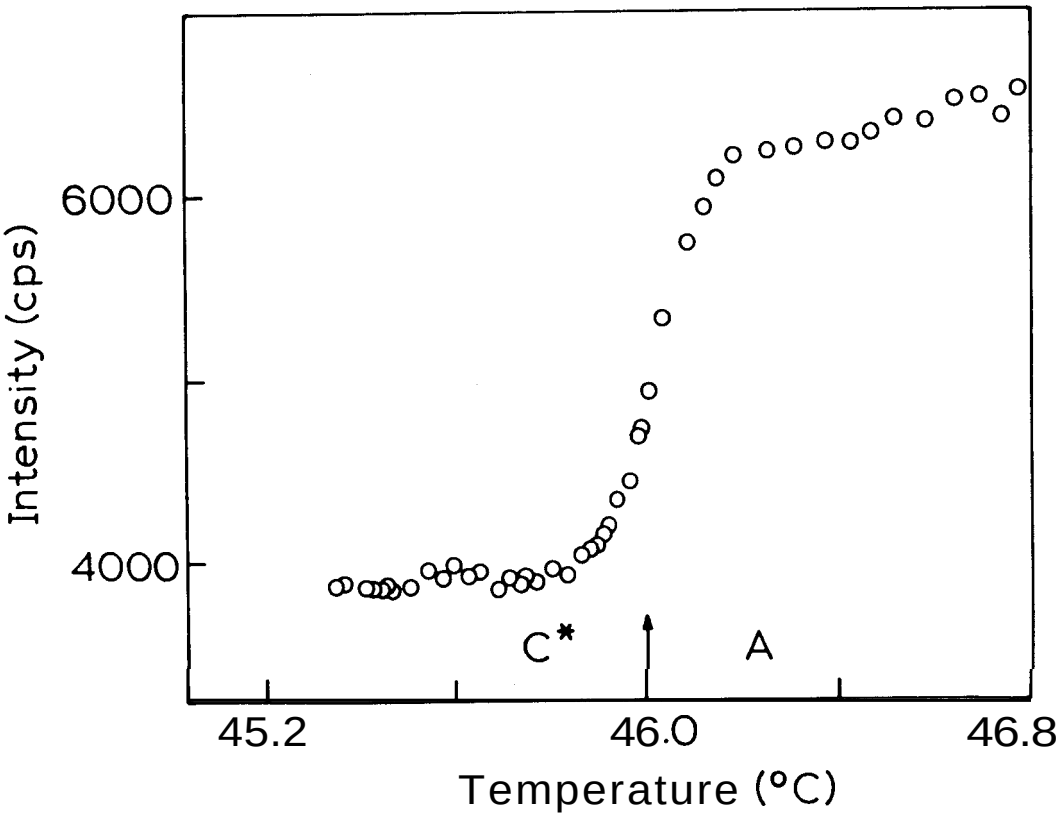

Figure **3.7:** (b) The intensity versus the temperature plot for X=15.0 shows a smooth variation across the transition.

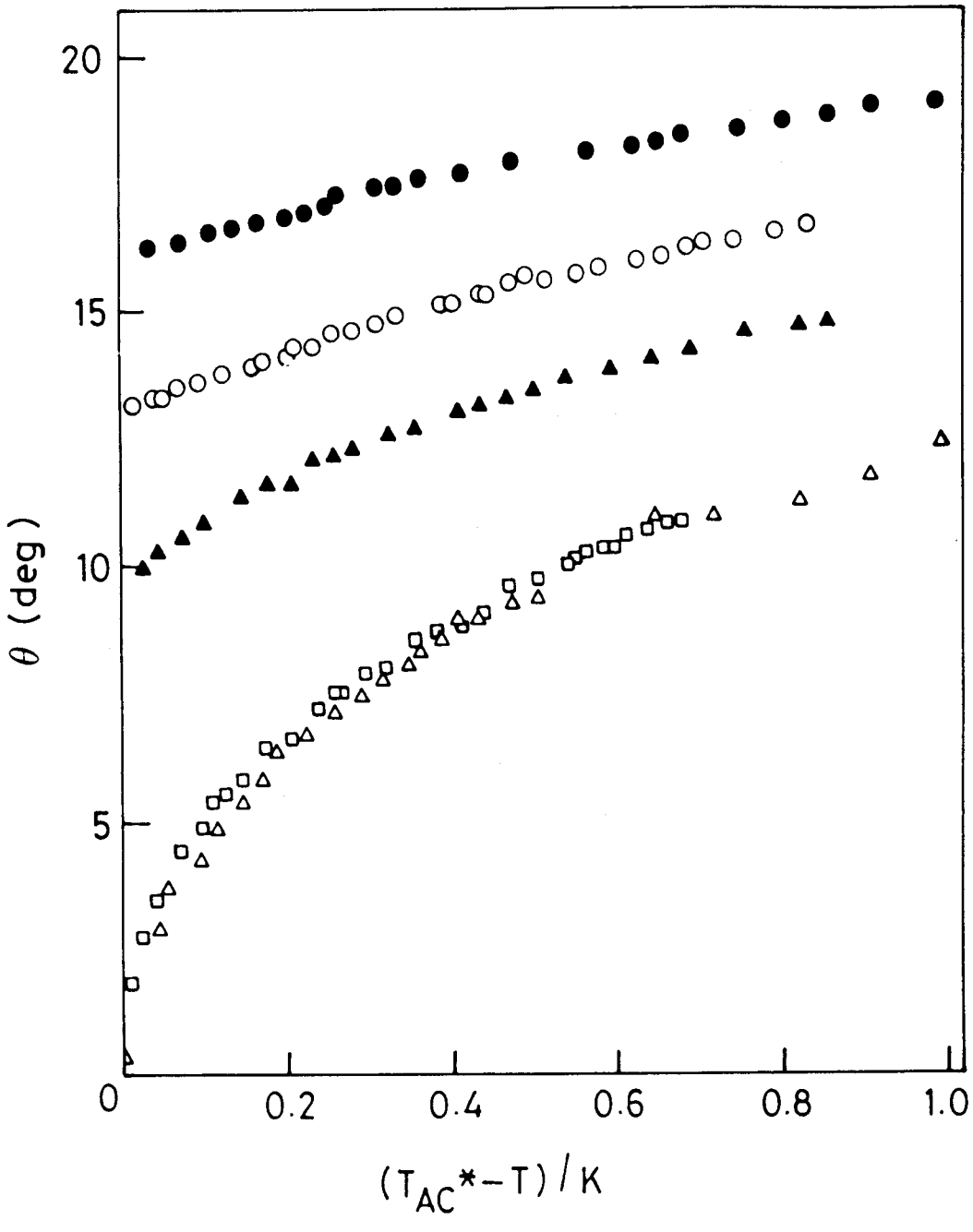

Figure 3.8: Variation of tilt angle θ as a function of temperature for MCP7OB and its mixtures with 7OPDOB. Tlie concentrations are X=0(•); X=5.15(o); X=9.68(▲); X=15.0(□) and X=19.4(△).

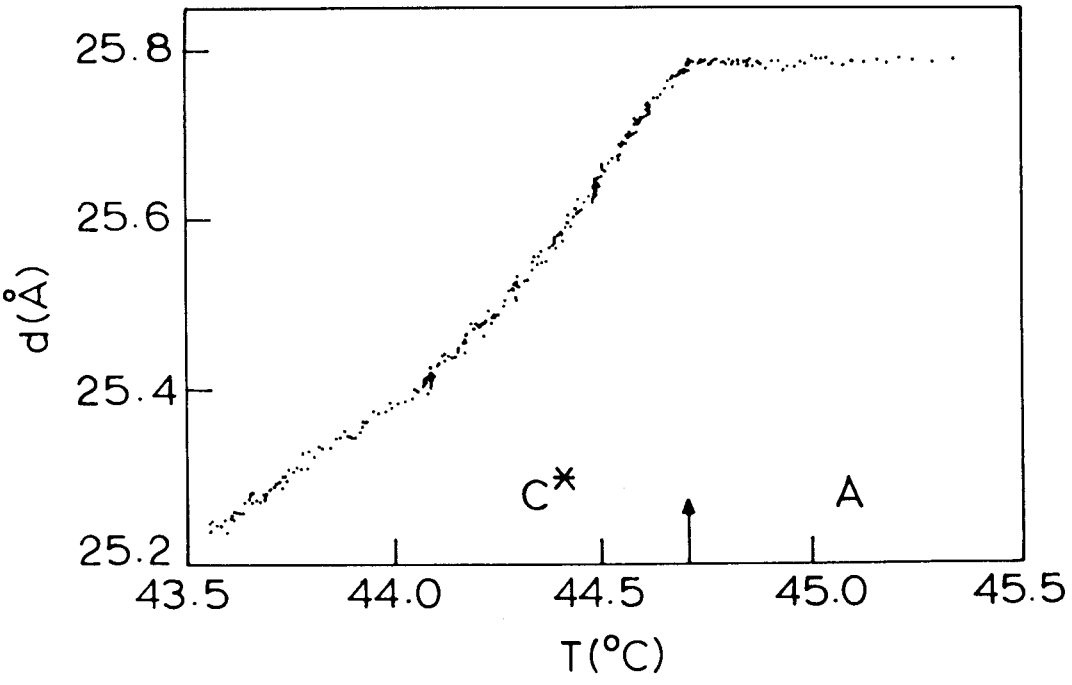

Figure 3.9: Layer spacing as a function of temperature for X=16.92.

3.3.1 Power law analysis

As discussed already, the thermal variation of 8 in the C* phase can be described by a simple power law of the type,

$$\theta = \theta_o t^{\beta} \tag{3.9}$$

where $t = \frac{T_{AC^*} - T}{T_{AC^*}}$, T_{AC^*} being the A-C* transition temperature and 8, is an amplitude term. β is the critical exponent for the thermal variation of the order parameter. The power law fitting was carried out using a non linear least square fit program with θ_o, T_{AC^*} and β being left as free parameters. When the fitting was done by taking the data over the entire temperature range (i.e., about 1 K from T_{AC^*}) in the case of each mixture the value of the critical exponent obtained was much lower compared to the MF exponent, **0.5.** For e.g., in the case of X=14.02 mixture, as shown in Figure **3.10** when the data upto 1K from the transition was fitted to the power law, the value of β obtained was **0.33** (which is close to XY class exponent). It was this kind of analysis which led the earlier experimenters to believe that this transition belongs to XY class. Therefore we have carried out the power law fitting analysis in a non trivial manner. For this a 'variable range' procedure was adopted, i.e., different limiting values of temperature (T_l) in the C* phase were chosen arbitrarily and in each case the data between T_l and T_{AC^*} were fitted to Equation **3.9** and the exponent β was calculated. For each concentration, about 15 limiting ranges, varying from as low as **40** mK to **1** K were chosen and the corresponding β was calculated for each range. The fitting carried out on the X=14.02 mixture data at four typical ranges, viz., **103, 250, 490** and **930** mK is shown in Figure **3.11.** The vertical

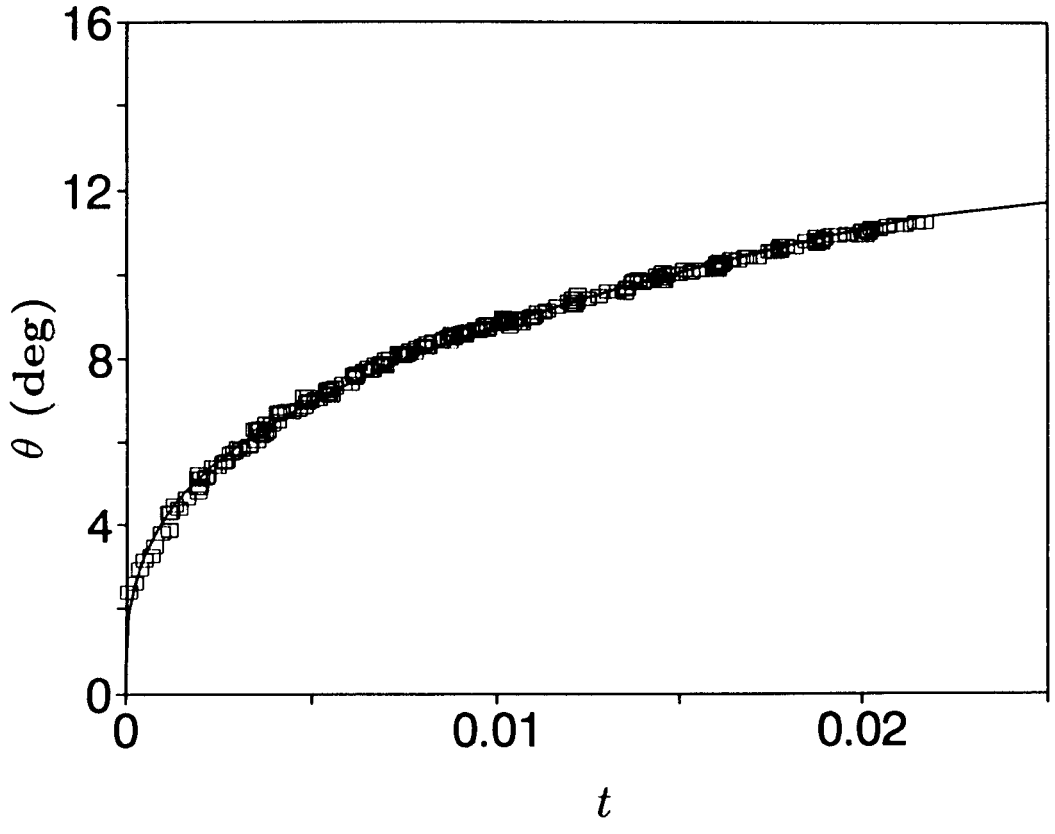

Figure 3.10: A single powerlaw fit to the entire data over a temperature range of 1K from the transition temperature for X=14.02 gives the exponent β as 0.33 (close to XY class exponent).

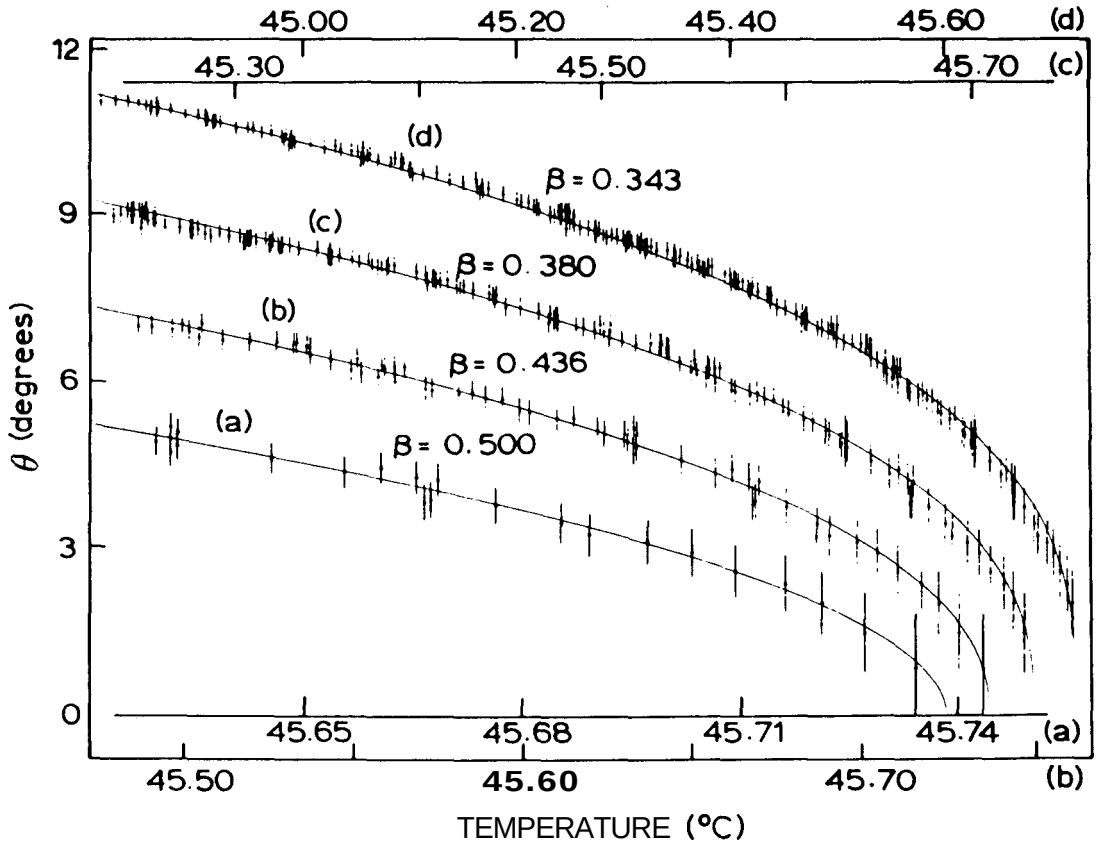

Figure 3.11: Tilt angle θ vs temperature plot in the C* phase for X=14.02. Solid lines are power law fit to the data, carried out for different temperture ranges viz., (a) 103 mK (b) **240** mK *(c)* **490** mK and (d) **930** mK. The corresponding β are marked in the figure. The vertical lines represent 3-standard deviation error to the tilt angle data.

lines represent the 3-standard deviation error on the tilt angle data. In each case the fitting is seen to be very good. Tlie β values calculated for different ranges are plotted against tlie fitting range in Figure 3.12. With decreasing range, β increases monotonically and for ranges $\leq$ 103 mK, it saturates at the MF value of 0.5, signifying a cross-over to asymptotic MF region. The observed trend in β is in agreement witli the predictions of tlie extended MF model. The theoretical plot[23] of the effective exponent (or cross-over exponent) β_{eff} versus reduced temperature given in Figure 3.13 looks similar to the experimental plot in Figure 3.12.

For all the mixtures, the analysis was carried out in a similar fashion by evaluating β over different T_l values (Figure 3.14). The figure shows that for the highest concentration, i.e., X=16.92, tlie temperature range (T_{MF}) over which β lias tlie true MF value of 0.5 is $\simeq$ 350 mK. With decreasing X, i.e., as the TCP is approached, T_{MF} also gets progressively smaller, until, finally for X=13.3 there appears to be, with in 30 mK, no MF region at all. This signifies that this concentration is at or extremely close to TCP. This is confirmed when β is evaluated over a wide range of temperature (T_{AC}^* - $T_l \simeq$ 10 K) in the C* phase. As the range of fitting is increased β indeed gets saturated at a value of 0.25 wliicli is the tricritical value[24] (see inset of Figure 3.14)

From Equation 3.9 we see that when θ versus t data is plotted on a double logarithmic scale, the data would fall on a straight line. Also, tlie slope of sucli a straiglit line directly gives the exponent β. Such a plot for X=15.49 (over T_{AC}^*-T =1 K temperature range) is shown in Figure 3.15. A straight line fits

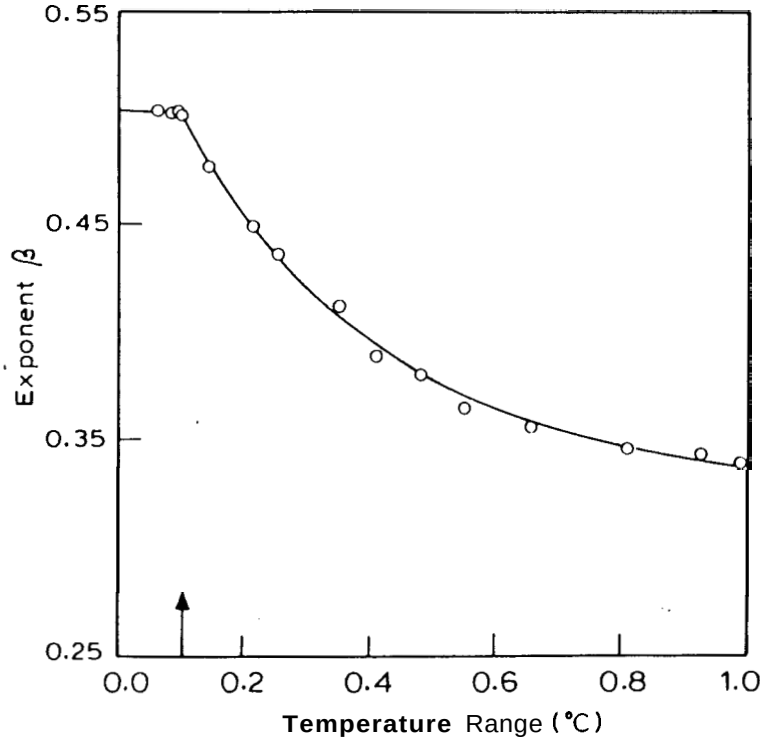

Figure **3.12:** β versus temperature range plot for X=14.02. As the temperature range decreases, β increases monotonically and for ranges $\leq$ **103** mK it saturates at the MF value of 0.5.

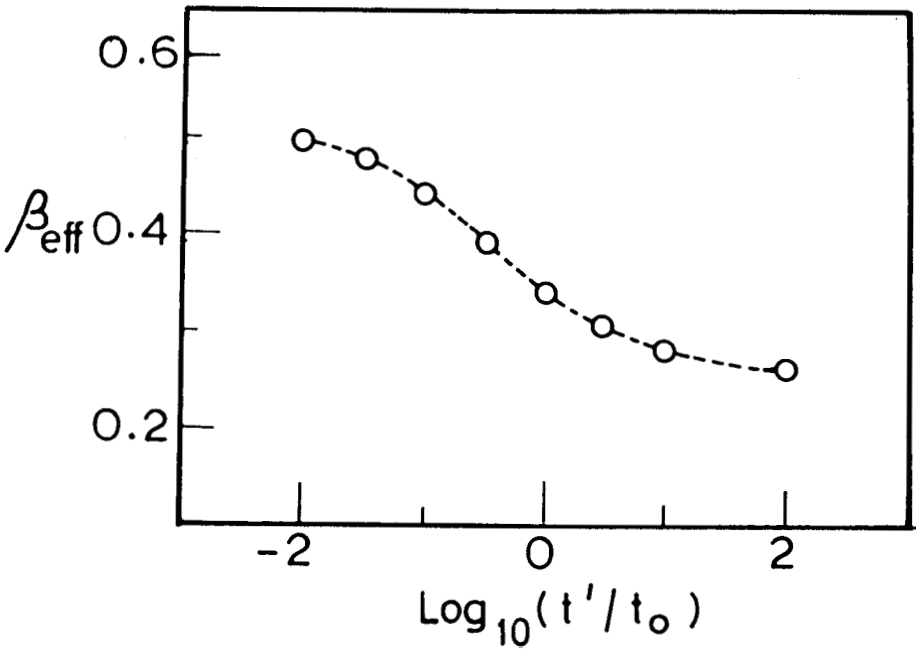

Figure **3.13:** The theoretical plot of the effective exponent versus the reduced temperature (from ref.[23]) looks very similar to Figure **3.12.**

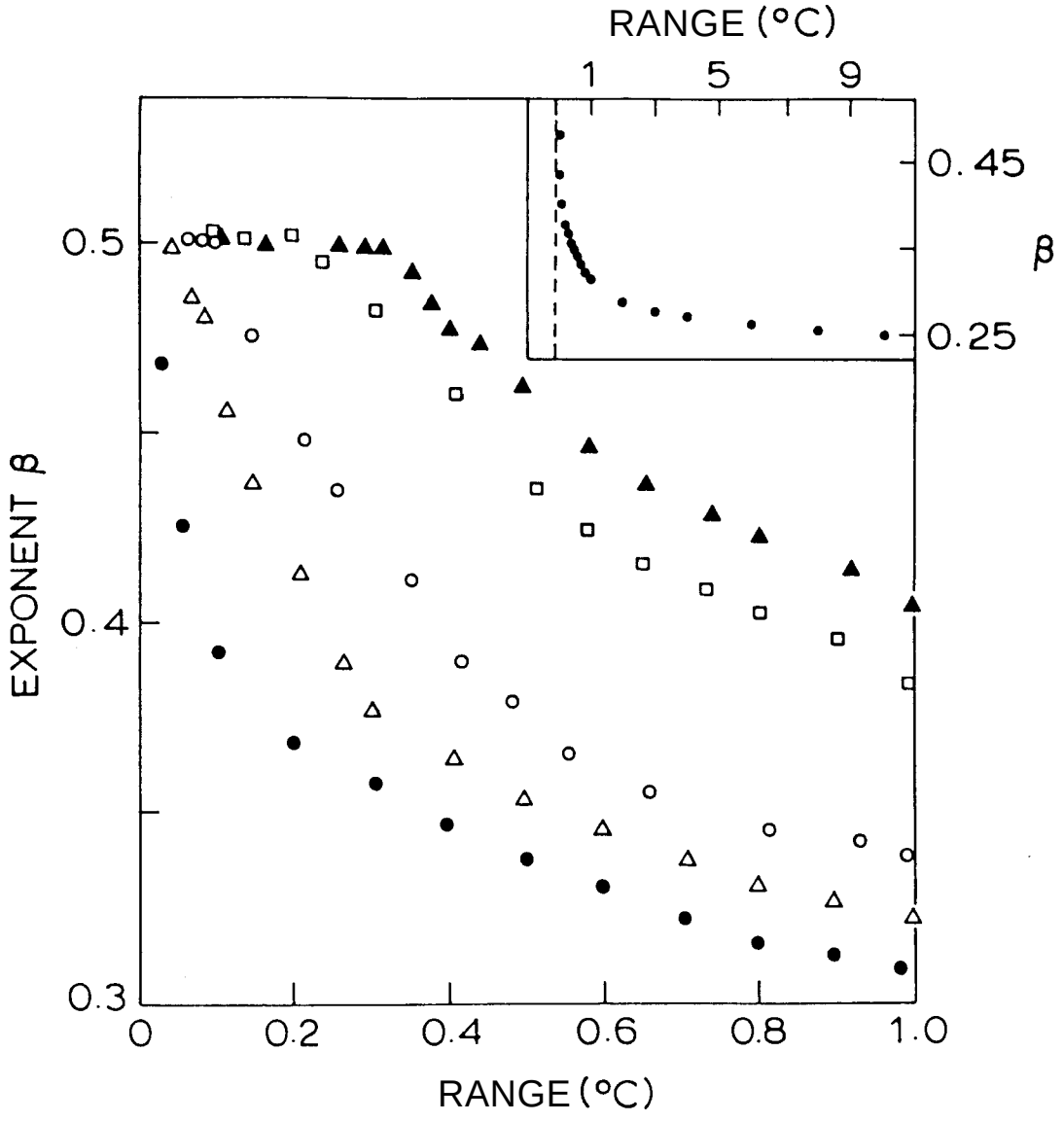

Figure **3.14:** Variation of β with temperature range for different mixtures of tlie MCP7OB – 7OPDOB binary system. The concentrations are **16.92** (filled triangles), **15.49** (squares), **14.02** (open circles), **13.6** (open triangles), and 13.3(filled circles). The MF region is seen to shrink with decreasing X. The mixture with X=13.3 for which no MF region is seen by power law fit is at or very close to the TCP. Inset: Plot of β vs range for this mixture over an extended temperature range ($\simeq$ **10** K) shows the saturation of β at the tricritical value of 0.25.

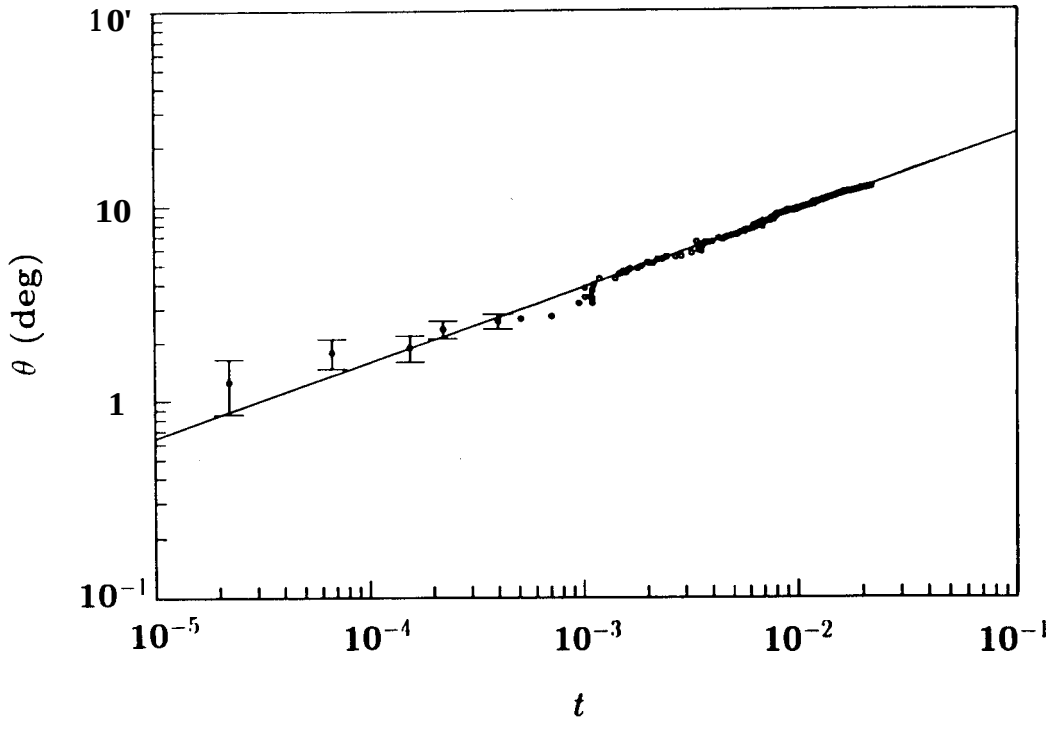

Figure 3.15: Double logarithmic plot of θ vs t for X=15.49. The straight line is the power law fit to the data and tlie slope of the straight line gives the exponent directly. $\beta = 0.388 \pm 0.003$. Tlie vertical lines are the 3-standard deviation error to the tilt angle.

tlle data well giving a slope = 0.388. But due to tlle inherent cross-over problem, this slope does not give the critical exponent β, but only its cross-over value. However, a similar plot for X=13.3, data upto T_{AC}^{*}-T $\simeq$ 10 K range, gives $\beta = 0.252 \pm 0.002$, tlle tricritical exponent (Figure 3.16).

3.3.2 Mean-field analysis

We have also analysed tlle data in tlle frame work of tlie extended mean-field model. An advantage of this method is that one can, not only get the value of tlle cross-over temperature t_o, but also obtain tlie different ratios of the Landau parameter, viz., b/c, b/a and a/c. Note that, by tlie very definition, tlle value of b and hence $t_o(=\frac{b^2}{nc})$ go to zero at the TCP.

From Equation 3.5

$$\theta = [R(1 + 3t/t_o)^{1/2} - 1]^{1/2} \tag{3.10}$$

wliere R = $(b/3c)$.

We have fitted the data for the different mixtures to Equation 3.10 by floating R, T_{AC}^{*} and t_o as free parameters. Tlie fits obtained in each case are plotted in Figures (3.17-3.21). It is seen that Equation 3.10 describes the data well in all the cases. For X=16.92 tlie value of t_o is 2.17 x10^{-3} (Figure 3.17) and as X decreases its value also decreases. For X=13.3 (Figure 3.21), the very small value of $t_o = 5 \times 10^{-5}$ (at TCP $t_o = 0$) supports tlie results of the power law analysis from which we identified this concentration to be at or very close to TCP. (A very similar kind of a mean-field TCP has been found[25] in tlie case of a chiral - racemic system at the racemate concentration).

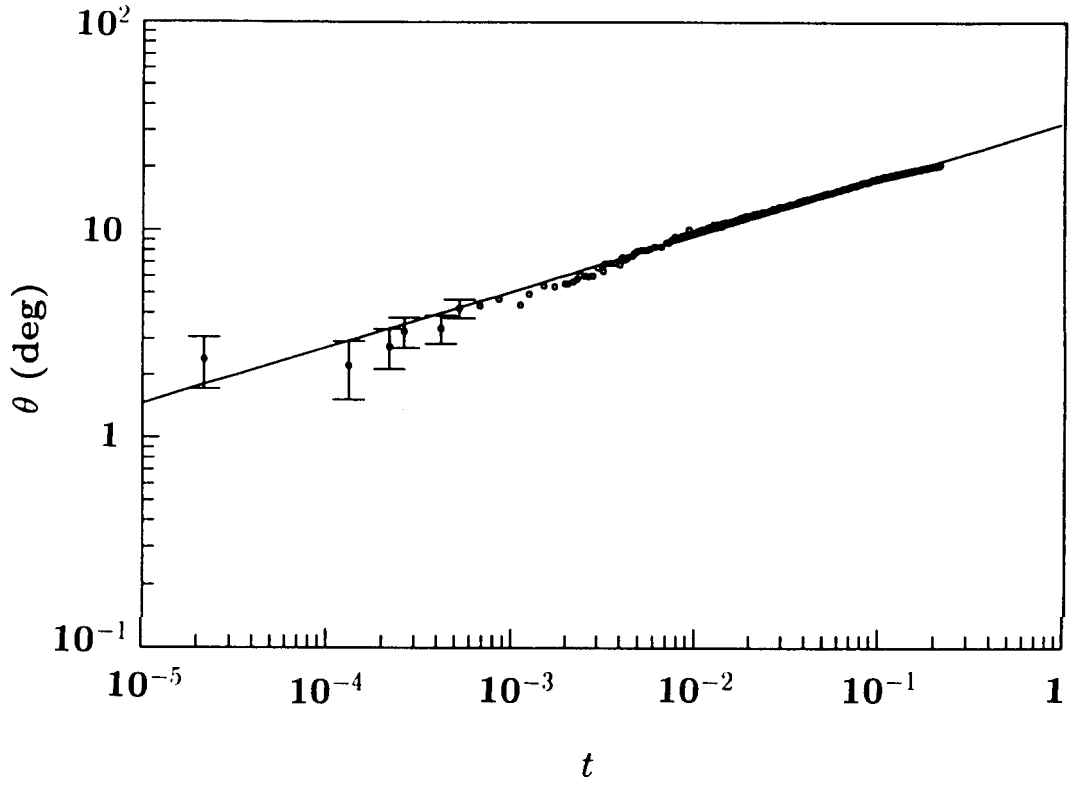

Figure 3.16: The plot of θ vs. t in double logarithmic scale for X=13.3. The slope of the straight line gives the tricritical exponent.(0.252±0.002)

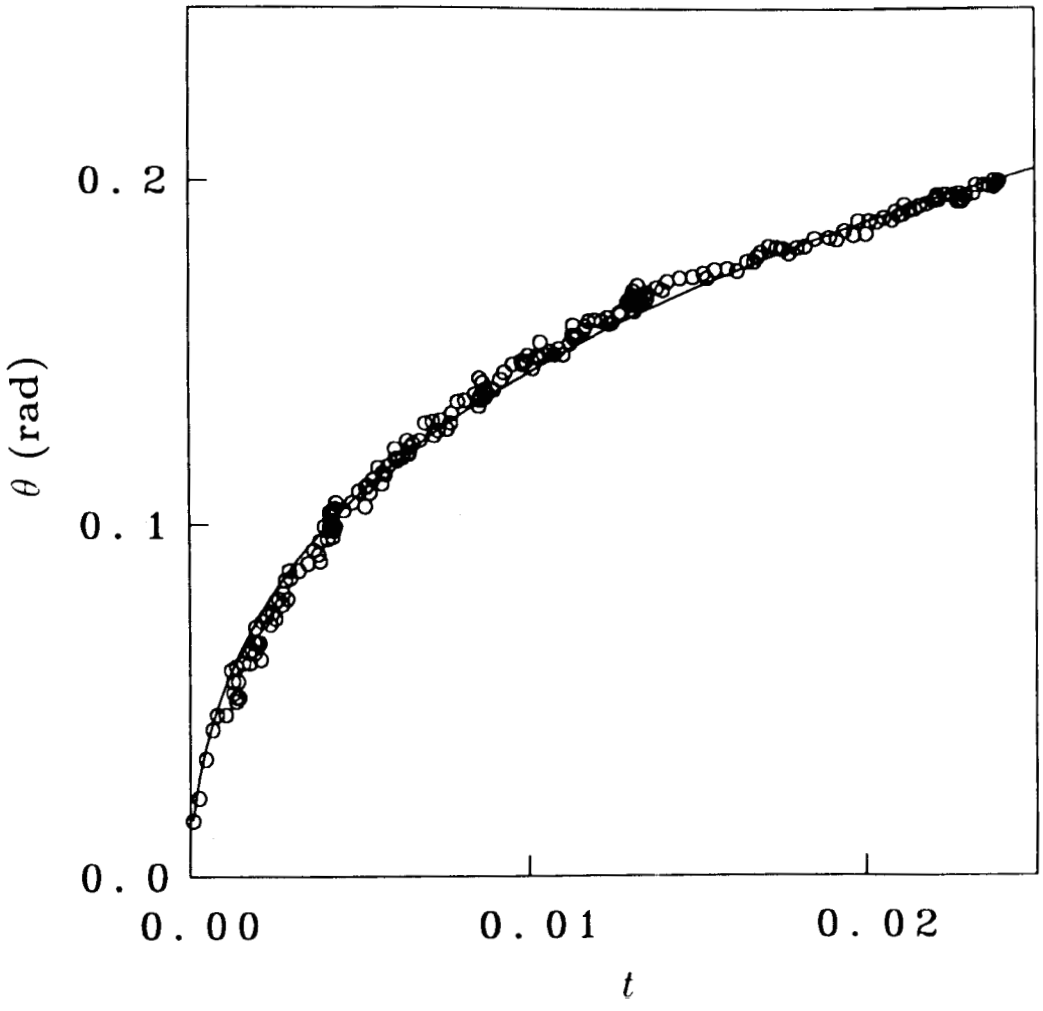

Figure 3.17: Fit of the tilt angle data for X=16.92 to Equation 3.10. The t_o obtained is 2.17×10^{-3}

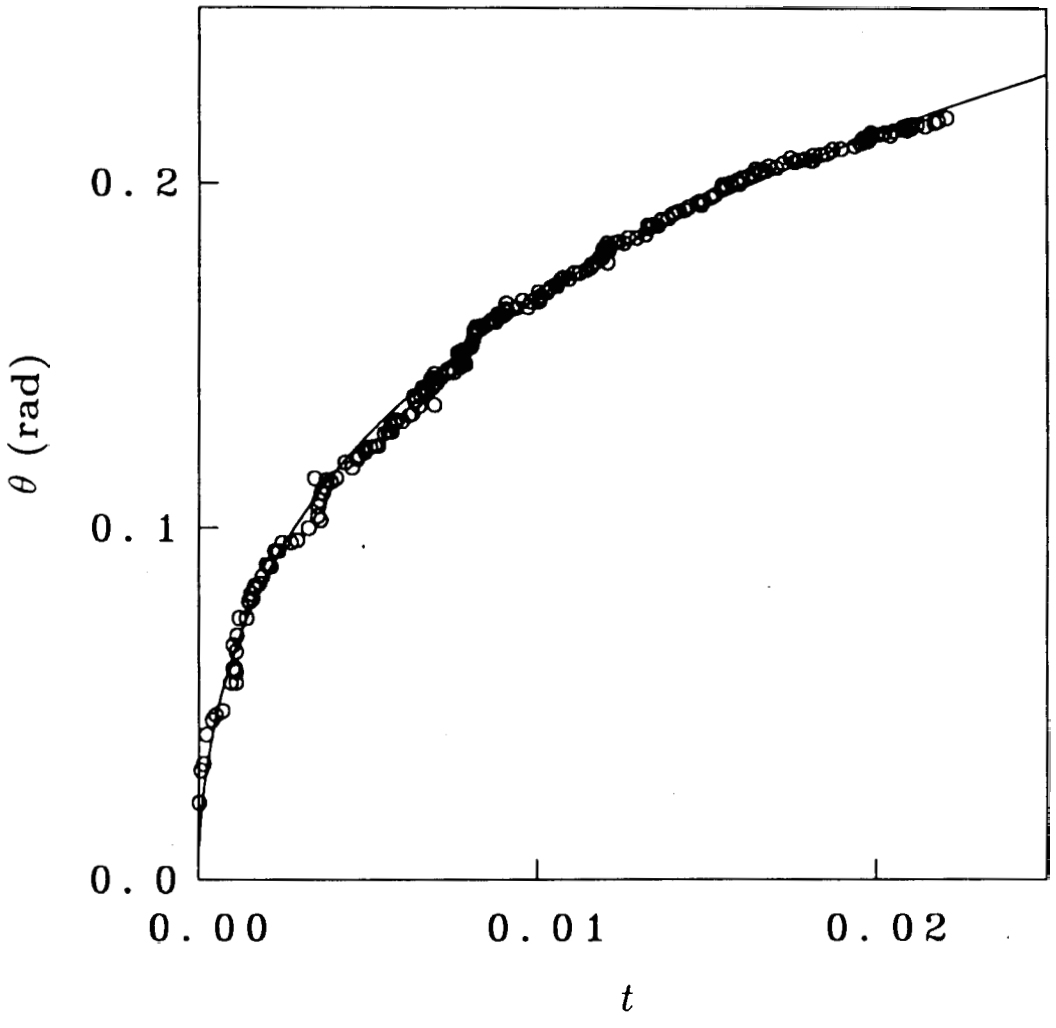

Figure 3.18: Extended mean-field fit **for** X=15.49. $t_o = 1.41 \times 10^{-3}$.

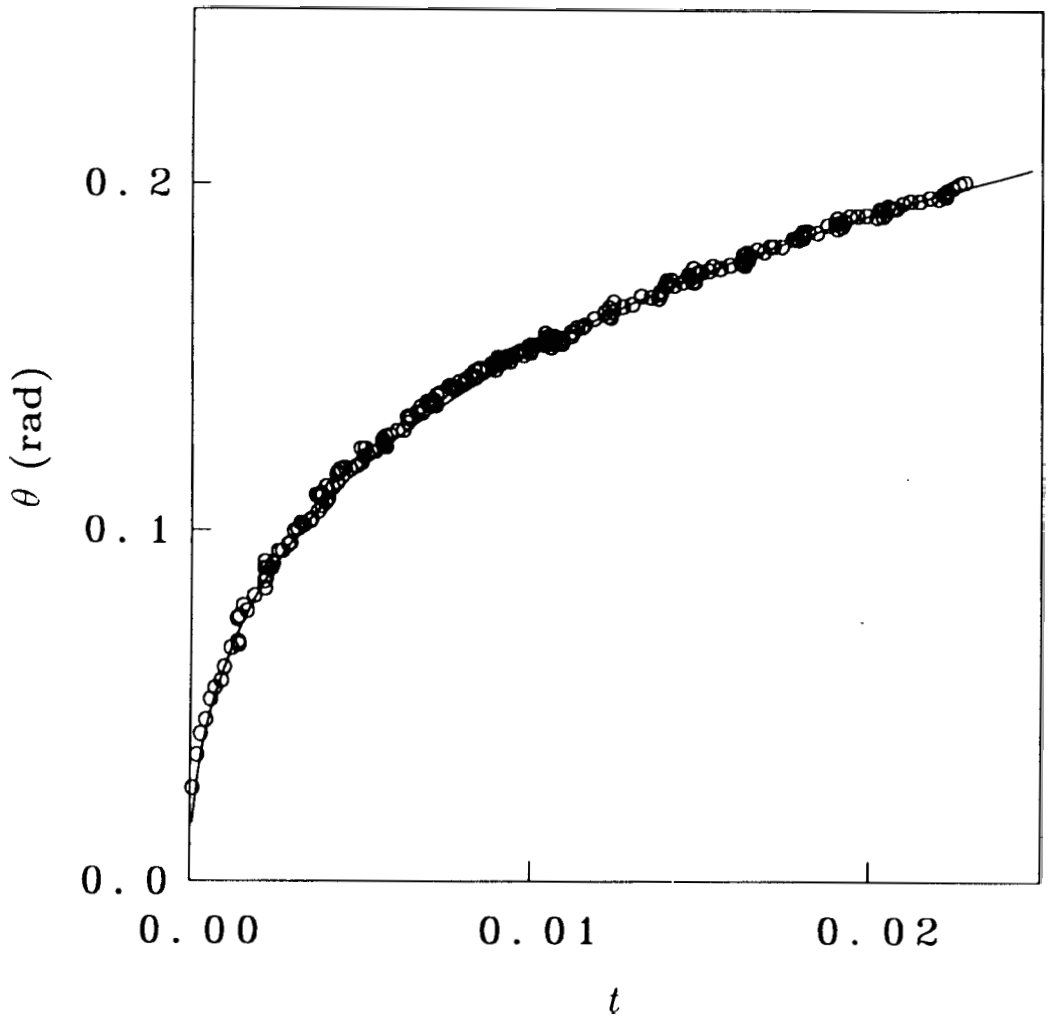

Figure 3.19: Extended mean-field fit for X=14.02. $t_o = 0.71 \times 10^{-3}$

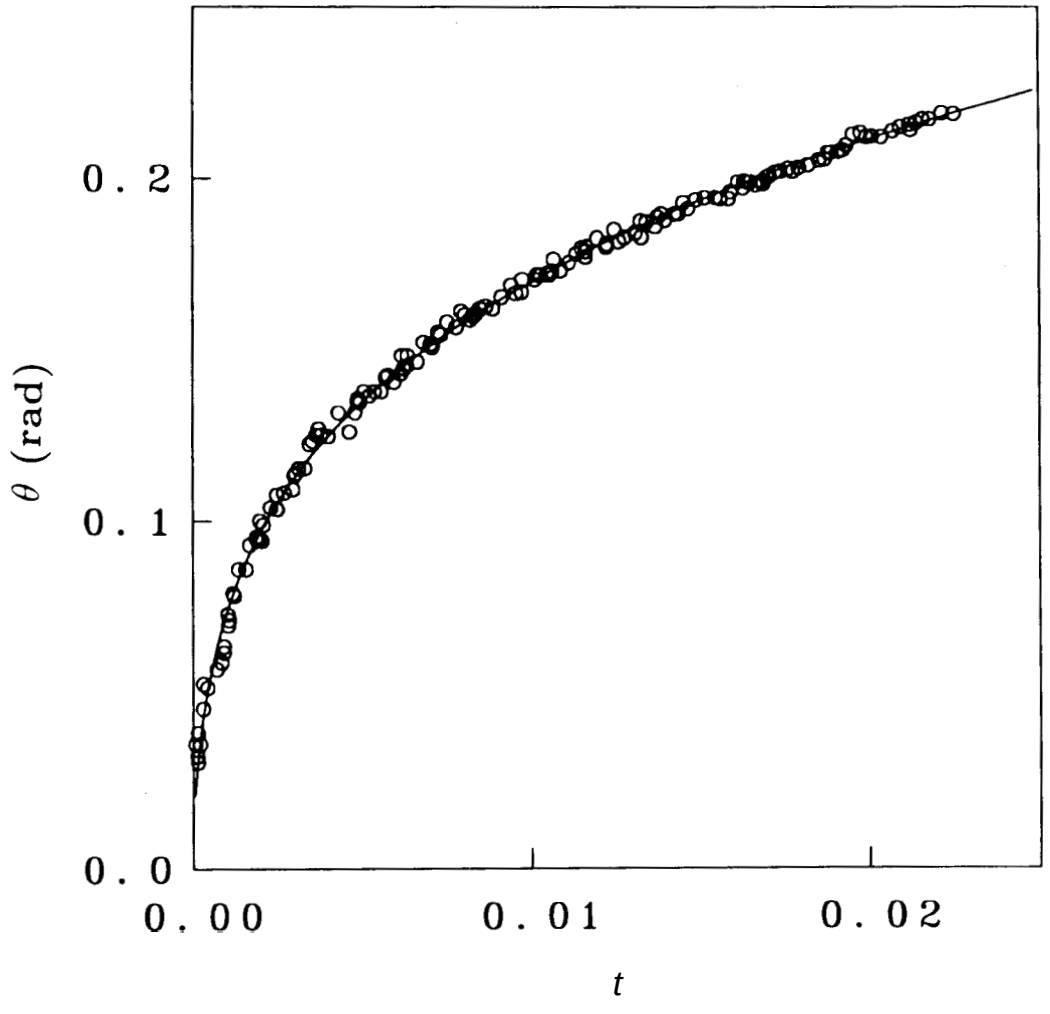

Figure 3.20: Extended mean-field fit for X=13.6. $t_o = 0.39 \times 10^{-3}$.

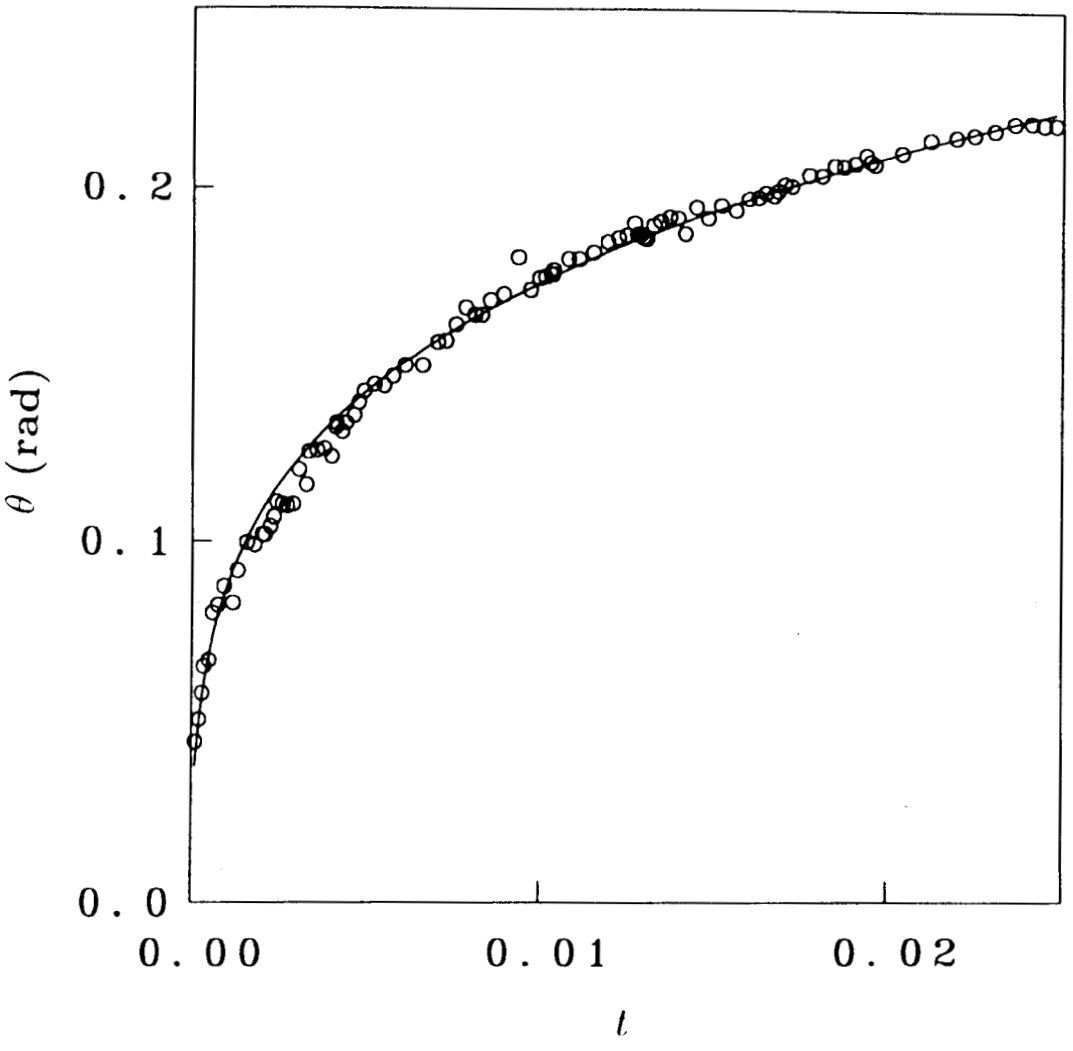

Figure 3.21: Extended mean-field fit for X=13.3. $t_o = 5 \times 10^{-5}$

The values of t_o obtained for different concentrations are tabulated in Table 3.2 along with t_{MF} (= $\frac{T_{MI.}}{T_{AC^*}}$) got from power law fits. As observed earlier, both t_o and t_{MF} decrease with decreasing concentration and vanish at TCP.

In Figure 3.22, we have plotted the partial T-X diagram, by also including a line representing the locus of the MF-TCP cross-over points. This plot, in fact is qualitatively similar to tlle theoretical 'catchment area' plot shown in Figure 3.3 (For ease of comparison the relevant portion of Figure 3.3 is shown in Figure 3.23).

As mentioned earlier, fitting done to Equation 3.10 also provides a way to calculate tlle ratio of Landau coefficients.

Now for a second order transition, from Equation 3.10,

$$R = (b/3c)$$

or

$$\frac{b}{c} = 3R \tag{3.11}$$

We also have,

$$t_o = \frac{b^2}{ac} \tag{3.12}$$

Equation **3.11** gives tlle ratio b/c. Dividing Equation 3.12 by Equation 3.11 we get the ratio b/a. Also dividing Equation 3.11 by b/a yields a/c. The values of the different ratios of Landau parameters for different mixtures on the second order side of the TCP are given in Table 3.3.

If the transition is first order, then b<0. In such a case from Equation 3.3 one gets, tlle jump in the tilt angle $\Delta\,\theta$ to be

$$\Delta\theta^2 = -\frac{3b}{4c}$$

Table **3.2:** The mean-field range(t_{MF}), cross-over temperature (t_o) and tlie range of tlie **A** phase for different mixtures of C7-7OPDOB system (T_{IA} is tlie isotropic-A transition temperature)

Mole percent	$10^3 t_{MF}$	$10^3 t_o$	T_{IA} - T_{AC^*} (°C)
16.92	1.03	2.17	15.5
15.49	0.72	1.41	14.8
14.02	0.31	0.71	14.1
13.60	0.13	0.39	13.7
13.30	...	0.05	13.4

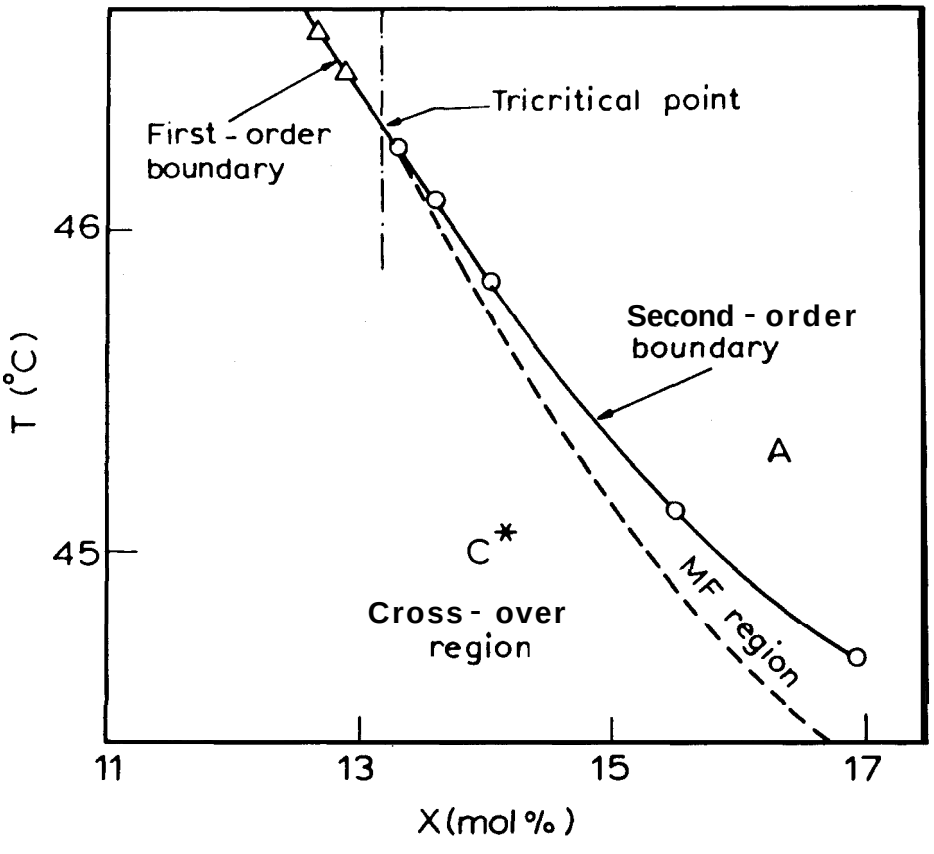

Figure **3.22:** Partial T-X diagram for MCP7OB-7OPDOB system showing tlic MF to tricritical cross over beliaviour near tlie A-C* TCP. The points on the phase boundary on the first order (triangles) as well as on the second order (circles) side of TCP liave been obtained from oytical microscopic studies. The dashed line representing the MF to tricritical cross-over temperature has been identified by power law fits. Notice that the MF region shrinks to zero at the TCP.

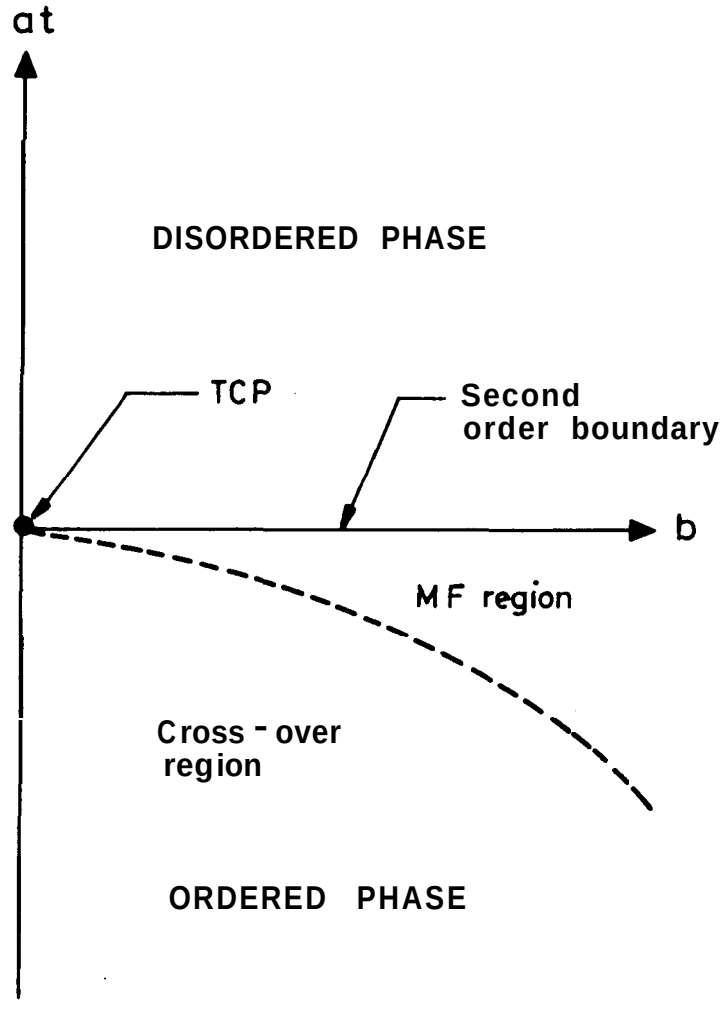

Figure **3.23:** Tricritical pliase diagram shown in Figure **3.3.** is plotted in order to compare with the experimental phase diagram shown in Figure **3.22.** The dashed line represents the MF to cross over region. Notice the similarity between the experimental and the tlieoretical curves.

Table **3.3:** The ratio of Landau parameters for different mixtures of C7-7OPDOB system

Mole percent	b/c rad^2	b/a rad^{-2} K	a/c rad^4 K^{-1}
16.92	0.087	0.025	0.284
15.49	0.084	0.017	0.199
14.02	0.042	0.017	0.406
13.60	0.035	0.011	0.318
13.30	0.010	0.005	0.491

$$\frac{b}{c} = -\frac{4}{3}\Delta\theta^2 \tag{3.13}$$

Using Equation 3.13 the $\frac{b}{C}$ ratio was calculated for mixtures on the first order side of tlie TCP. Figure 3.24 sliows tlie plot of $\frac{b}{c}$ versus concentration (X). In conformity with the t_o and t_{MF} data tlie b/c ratio also goes to zero at X=13.3, tlie TCP concentration. It is interesting to note here tliat a similar curve (shown in Figure 3.25) has been seen in the case of a ferroelectric semiconductor alloy[26].

Thus, tlie results of our high resolution X-ray measurements of the tilt angle in tlie MCPSOB - SOPDOB binary system establish tlie existence of a TCP on tlie A-C* transition line. Detailed analysis has brought out many associated features:

1. Mean-field to tricritical cross-over beliaviour.

2. The Mean-field range shrinking to zero at the TCP.

Tlie analysis demonstrates tlie power of tlie range shrinking method in obtaining the true value of tlie order parameter critical exponent. Further, the conclusions drawn are found to be in good agreement with tliose obtained from the extended mean-field model.

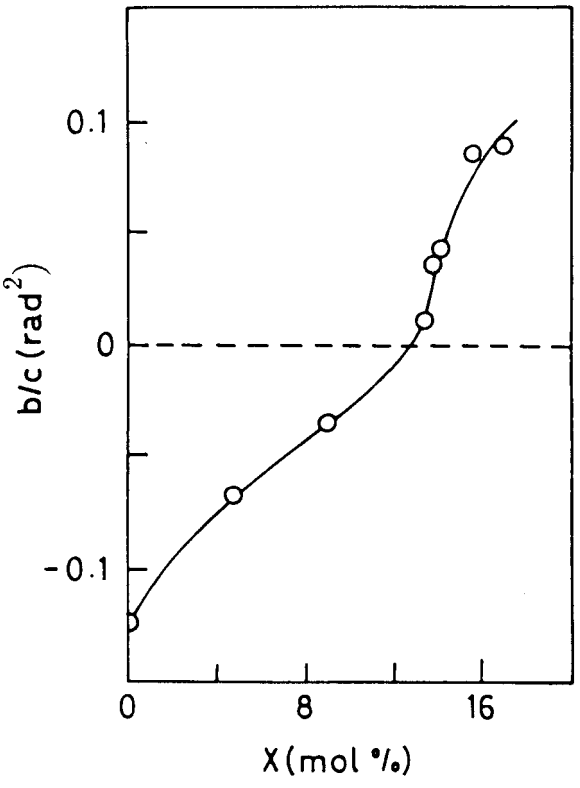

Figure 3.24: Plot of the ratio b/c against the concentration X. b goes to zero at the TCP. The solid line is just a guide to the eye.

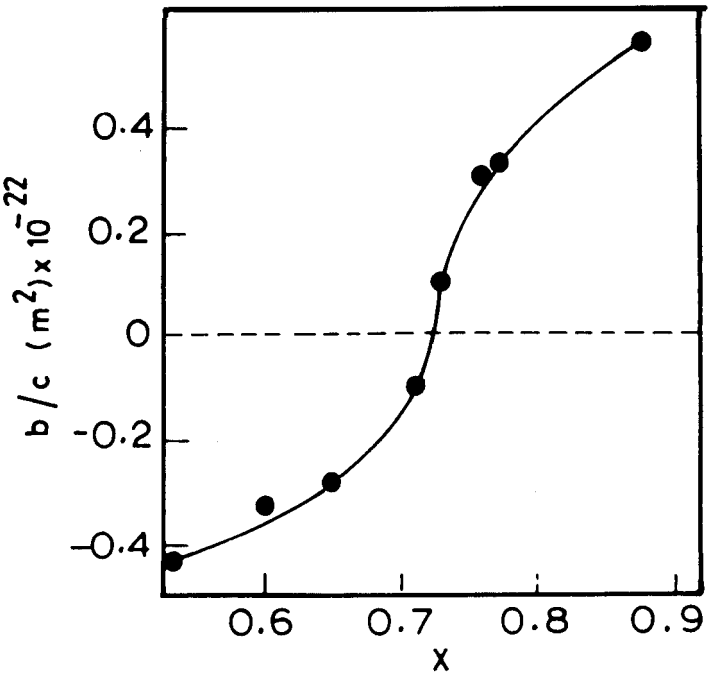

Figure 3.25: A plot, b/c us X in the case of a semiconducter alloy ref.[26]. The plot looks very similar to the plot shown in Figure 3.24.

References

[1] R. B. Griffitlis, *Phys. Rev. Lett. 24,* 715 (1970).

[2] D. L. Johnson, C. Maze, E. Oppenheim and R. Reynolds, *Phys. Rev. Lett.* 34, 1143 (1975).

[3] P. H. Keyes, H. T. Weston and W. B. Daniels, *Phys. Rev. Lett.* 31, *628* (1973).

[4] R. Shashidhar and S. Cliandrasekliar, *J. de Physique* 36, C1-49 (1975).

[5] L. D. Landau and E. M. Lifsliitz, *Statistical Physics,* Vol.5, Pergamon Press, Oxford (1980).

[6] R. B. Griffiths, *Phys. Rev.* B **7,** 545 (1973).

[7] E. H. Graf, D. H. Lee and J. D. Reppy, *Phys. Rev. Lett* 19, 417 (1967).

[S] C. Vettier, H. L. Alberts and D. Bloch, *Phys. Rev. Lett.* 31, 144 (1973); W. P. Wolf, D. P. Landau, B. E. Keen and B. Schneider, *Phys. Rev.* B *5,* 4472 (1972).

[9] C. W. Garland and B. B. Weiner, *Phys. Rev.* B 3, 1034 (1971); W. B. Yelon, D. E. Cox, P. J. Kortman and W. B. Daniels, *Phys. Rev.* **B9**, 4843 (1974); G. Dolino, J. P. Pique and M. Vallade J. *Physique Lett. 40,* L-303 (1979).

[10] R. Clarke and L. Benguigui, J. *Phys. C* **10**, 1963 (1977)

[11] A. Samara, *Ferroelectrics* **9,** 209 (1975); P. S. Percy, *Phys. Rev. Lett.* 35, 1581 (1975).

[12] V. H. Schmidt, A. B. Western and A. G. Baker, Phys. Rev. Lett. 37, 839 (1976).

[13] P. G. de Gennes, Mol. *Cryst.* Liq. *Cryst.* **21**, 49 (1973).

[14] R. A. Wise, D. H. Smith and J. W. Doane, Phys. Rev. ***A*** 7, 1366 (1973).

[15] D. Gullion and A. Sloulios, **J.** Physique 38, 79 (1977).

[16] S. Meiboom and R. C. Hewitt, Phys. Rev. ***A*** 15, 2444 (1977)

[17] Y. Galerne, Phys. Rev. ***A*** 24, 2284 (1981).

[18] S. Kumar, Phys. Rev. ***A*** 23, 3207 (1981).

[19] C. R. Safinya, M. Kaplan, J. Als-Nielsen, R. J. Bigeneau, D. Davidov, J. D. Litster, D. L. Johnson and M. E. Neubert Phys. Rev. B 21, 4149 (1980); R. J. Birgeneau, C. W. Garland, A. R. Kortan, J. D. Litster, M. Meichle, B. M. Ocko, C. Rosenblatt, L. J. Yu and J. W. Goodby, Phys. Rev. ***A*** 27, 1251 (1983); M. Meichle and C. W. Garland, Phys. Rev. ***A*** 27, 2624 (1983).

[20] V. L. Ginzburg, *Sov.* Phys. Solid State 2, 1824 (1960).

[21] J. D. Litster, J. Als-Nielsen, R. J. Birgeneau, S. S. Dana, D. Davidov, F. Garcia-Golding, M. Kaplan, C. R. Safinya and R. Schaetzing, **J.** Physique, 40, C3-339 (1979).

[22] C. C. Huang and J. M. Viner, Phys. Rev. ***A*** 25, 3385 (1982).

[23] C. C. Huang and J. M. Viner, Liquid *Crystals* and *Ordered* Fluids, edited by A. C. Griffin and J. F. Johnson ,Plenum, New York, Vo1.4, p.643, (1984).

[24] See for eg.,S. Chandrasekhar, *Liquid Crystals*, Cambridge University Press, (1992); M. Plischke and B. Bergersen, *Equilibrium* Statistical Physics, Prentice Hall Advanced Reference Series, (1989).

[25] H. Y. Liu, C. C. Huang, Ch. Bahr and G. Heppke, Phys. *Rev. Lett.* **61, 345** (1988).

[26] R. Clarke, *Phys.* *Rev.* B 18, 1920 (1978).